On the Inertia of Future More-Electronics Power Systems

Jingyang Fang, *Student Member, IEEE*, Hongchang Li, *Member, IEEE*, Yi Tang, *Senior Member, IEEE*, and Frede Blaabjerg, *Fellow, IEEE*

***Abstract*— Inertia plays a vital role in maintaining the frequency stability of power systems. However, the increase of power electronics-based renewable generation can dramatically reduce the inertia levels of modern power systems. This issue has already challenged the control and stability of small-scale power systems. It will soon be faced by larger power systems as the trend of large-scale renewable integration continues. In view of the urgent demand for addressing the inertia concern, this paper presents a comprehensive review of inertia enhancement methods covering both proven techniques and emerging ones and also studies the effect of inertia on frequency control. Among those proven techniques, the inertia emulation by wind turbines has successfully demonstrated its effectiveness and will receive widespread adoptions. For the emerging techniques, the virtual inertia generated by the dc-link capacitors of power converters has a great potential due to its low cost. The same concept of inertia emulation can also be applied to ultracapacitors. In addition, batteries will serve as an alternative inertia supplier, and the relevant technical challenges as well as the solutions are discussed in this paper. In future power systems where most of the generators and loads are connected via power electronics, virtual synchronous machines will gradually take over the responsibility of inertia support. In general, it is concluded that advances in semiconductors and control promise to make power electronics an enabling technology for inertia control in future power systems.**

***Index Terms*— Batteries, control, energy storage, inertia, power electronics, power systems, renewable energy sources (RESs), ultracapacitors, virtual synchronous machines (VSMs).**

I. Introduction

TECHNICAL factors contributing to the eventual adoption of alternating current (ac) over direct current (dc) in the 1890s comprise a marriage of the developments of practical transformers and polyphase systems. Transformers play a vital role as they enable ac power to be easily transformed and transmitted at high-voltage levels [1]. Along with the polyphase systems invented by Tesla [2], ac power becomes even more attractive. As a fundamental health indicator of ac power systems, the grid frequency reveals the degree of balancing between generation and demand. Referring to Fig. 1, the grid frequency will decline as long as the demand exceeds the generation, and vice versa. Power systems in the majority of the world share a standard frequency of 50 Hz, except for the Americans and parts of Asia, where the nominal frequency is 60 Hz. The complete worldwide standardization seems economically unattractive, and there is no great technical reason to prefer one over the other [3]. Frequencies as high as 400 Hz are used in small-scale weight-sensitive systems, such as aircraft, submarine, and computer power supply systems, mainly for reducing the size of transformers and filters. On the contrary, traction power systems for railways operate at low frequencies (e.g., 16.67 and 25 Hz in several countries in Europe and the U.S., respectively) due to historical reasons, mainly related to the use of dc-machine-based traction motors, and such railway power systems are interconnected with 50 Hz (or 60 Hz) main power systems through either rotary frequency converters or static power electronic converters.

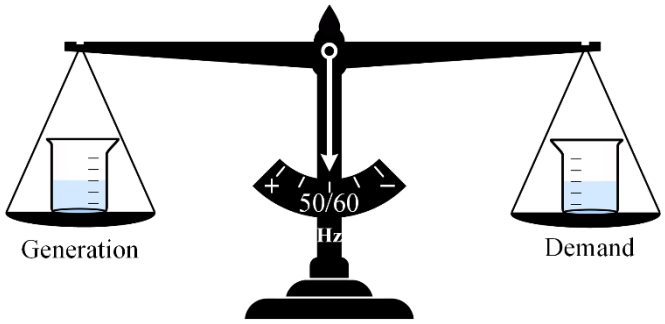

Fig. 1. Fundamental principle of frequency control in power systems.

Frequency control, i.e., the balance of generation and demand, is of great importance and has been identified as a high priority area by many power system operators [4]–[7]. For example, the National Grid in Great Britain spends around 160–170 million pounds annually on frequency control [8]. Ideally, the grid frequency should always stay at its nominal value. Unfortunately, ever-changing load and generation profiles will cause frequency deviations. The operation of

Manuscript received April 3, 2018; revised July 17, 2018 and September 11, 2018; accepted October 18, 2018. Date of publication October 24, 2018; date of current version November 4, 2019. This work was supported by National Research Foundation, Prime Minister's Office, Singapore, through the Energy Program and Energy Market Authority under EP Award NRF2015EWT-EIRP002-007. The paper has been presented in part in [116]. Recommended for publication by Associate Editor Carl N. M. Ho. *(Corresponding author: Yi Tang.)*

J. Fang and Y. Tang are with the School of Electrical and Electronic Engineering, Nanyang Technological University, Singapore 639798 (e-mail: jfang006@e.ntu.edu.sg; yitang@ntu.edu.sg).

H. Li is with the Energy Research Institute, Nanyang Technological University, Singapore 639798 (e-mail: hongchangli@ntu.edu.sg).

F. Blaabjerg is with the Department of Energy Technology, Aalborg University, Aalborg 9220, Denmark (e-mail: fbl@et.aau.dk).

Color versions of one or more of the figures in this article are available online at http://ieeexplore.ieee.org.

Digital Object Identifier 10.1109/JESTPE.2018.2877766

TABLE I
STANDARDS ON FREQUENCY CONTROL PRESCRIBED BY INTERNATIONAL GRID CODES

Country/region	Australia [11]	China [12]	Europe [13]	Great Britain [6]	Japan [14]	North America [15]	Singapore [7]
Nominal frequency	50 Hz	50 Hz	50 Hz	50 Hz	50/60 Hz	60 Hz	50 Hz
Normal operating frequency band	Interconnected system: ±0.15 Hz Islanded system: ±0.5 Hz	System ≥ 3 GW: ±0.2 Hz System < 3 GW: ±0.5 Hz	±0.2 Hz	±0.5 Hz Target frequency band: ±0.05 Hz	±0.2 Hz or ±0.3 Hz	Targeted frequency band: Eastern Interconnection: ±0.018 Hz Western Interconnection: ±0.0228 Hz Texas Interconnection: ±0.030 Hz Quebec Interconnection: ±0.021 Hz	±0.2 Hz
Operational frequency tolerance band	49−51 Hz Extreme frequency tolerance band: 47−52 Hz	49−51 Hz	49.2−50.8 Hz	49−51 Hz Under-frequency load shedding: 48.8 Hz	−	Under-frequency load shedding: Eastern Interconnection: 59.5 Hz Western Interconnection: 59.5 Hz Texas Interconnection: 59.3 Hz Quebec Interconnection: 58.5 Hz	Under-frequency load shedding: 49.7 Hz

generating units at a low frequency may impose vibratory stresses on the turbine blades and reduce the outputs of boiler feed pumps or fans [9]. To guard against low-frequency operations, under-frequency protective relays are normally involved so that generators will be tripped off when the frequency decline is excessive. Therefore, tripping of generation, cascading outages, or even isolation of areas and formation of electrical islands may happen as the results of an ineffective frequency control [9]. Grid codes all over the world attempt to avoid such undesirable effects by prescribing standards on frequency control, as tabulated in Table I [4]–[7], [10]–[15], where the normal operating frequency band limits long-term frequency deviations, while the operational frequency tolerance band sets the allowable ranges for instantaneous frequency deviations [15]. Instead of providing frequency tolerance bands, countries like Singapore fix the thresholds for under-frequency load shedding [7]. Upon reaching these thresholds, loads will partially be shed, thus helping to stabilize the grid frequency.

As required by grid codes, the power balance between generation and demand following a frequency event must be reached in a fast-enough way such that frequency excursions remain within the bands in Table I. For illustration, Fig. 2 shows a typical frequency response trace following a tripping of generator event, where f_r represents the grid frequency, Δf_r denotes the frequency deviation or change, and the frequency nadir refers to the minimum frequency point. During the frequency event, the primary control must arrest the fast frequency decline, i.e., the frequency nadir, in the timescale of seconds, and then the secondary control restores the frequency in several minutes or tens of minutes [15]. The effect of the primary control is contributed by both frequency droop and inertia [16]. Inertia is an inherent property of synchronous generators (SGs). When the frequency drops, SGs autonomously turn slower and release the kinetic energy stored in their rotors to slow down frequency deviations, thus helping to mitigate the frequency nadir. As the penetration levels of renewable energy sources (RESs) grow, inertia decreases.

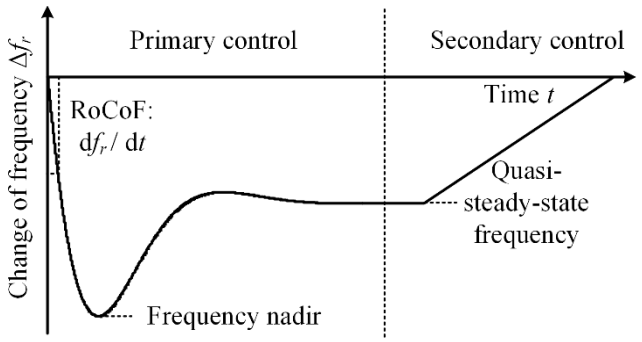

Fig. 2. Frequency response trace following a tripping of generator event. (RoCoF: rate of change of frequency).

This is because RESs are normally coupled to the power grid through static power electronics devices, which do not possess any inertia [17]–[21]. The decreased inertia deteriorates the frequency nadir and threatens the system stability and reliability. Therefore, great efforts should be attached to the improvement of inertia.

The reduction of inertia in future power systems will challenge the regulation of the time derivative of frequency, i.e., the rate of change of frequency (RoCoF). When exposed to high-RoCoF events, generating units are subject to the risk of pole slipping and catastrophic failure. Reference [22] indicates that pole slipping normally occurs when the RoCoF ranges from 1.5 to 2 Hz/s (over a 500-ms rolling window). As a result, high-RoCoF events may cause the protective tripping of generating units. In addition, in some jurisdictions, such as Ireland/North Ireland, the anti-islanding protection has been designed based on the detection of the RoCoF [8], and hence, it is quite necessary to prevent excessive RoCoF levels. The capability of mitigating RoCoF levels is another benefit of inertia. For power systems with high inertia, the grid frequency changes slowly, and thus, it can easily be stabilized. However, the ever-decreasing inertia brings in concerns of high-RoCoF levels (>0.5 Hz/s), particularly for small-scale power systems

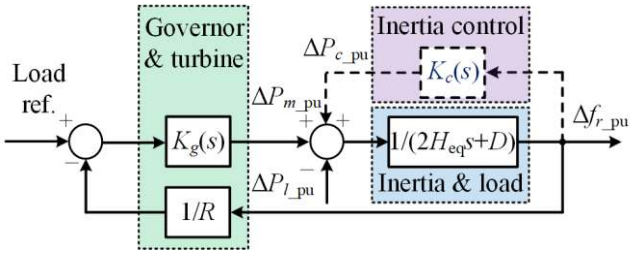

Fig. 3. Frequency control framework of single-area power systems.

without any ac interconnection, e.g., Ireland and Great Britain systems [8].

Many projects aiming to overcome the above-mentioned challenges were initiated, such as the enhanced frequency control capability (EFCC)/SMART Frequency Control Project and Future Power System Security Program project established by National Grid and Australia Energy Market Operator, respectively [23], [24]. In view of the urgent demand for improving the inertia in future more-electronics power systems, this paper provides a comprehensive review of inertia enhancement methods. The remaining of this paper begins with the analysis of the inertia effect on frequency control in Section II. Following that, the proven and emerging techniques are detailed in Sections III and IV, respectively. Their technical challenges are discussed in Section V. This is followed by a brief outlook of the future trend given in Section VI. Finally, Section VII concludes the main contributions of this paper.

II. Effect of Inertia on Frequency Control

Before demonstrating the effect of inertia, a standard frequency control framework of single-area power systems is shown schematically in Fig. 3, where R is referred to as the speed regulation or droop, which, together with $K_g(s)$, can model the speed governor and turbine of thermal, hydraulic, and nuclear power plants [9]. D with a typical value of 1–2 denotes the load-damping constant. Physically, it means the change in the absorbed power of motor loads with the frequency due to the change in motor speeds [9]. ΔP_{m_pu} and ΔP_{l_pu} stand for the mechanical power change and non-frequency-sensitive load change, respectively, where the subscript pu and prefix Δ are per unit and perturbed notations, respectively. ΔP_{c_pu} and $K_c(s)$ are related to inertia control and will be discussed later.

To evaluate the inertia contributions of individual SGs, the inertia constant H is defined as the ratio of the kinetic energy (W·s) at the rated speed to the system base power (VA), expressed as $H = J\omega_{0m}^2/(2VA_{\text{base}})$, where J denotes the moment of inertia, ω_{0m} represents the rated angular velocity of rotors, and VA_{base} stands for the rated power of SGs [9]. For power systems with multiple SGs, H_{eq} is defined to represent the equivalent power system inertia constant. Fig. 4 visualizes the effect of H_{eq} on frequency control. It is rather obvious that the case with the increased H_{eq} achieves an effective improvement of the frequency nadir. Moreover, increasing H_{eq} also helps to mitigate the RoCoF. The mechanism for inertia enhancement is essentially increasing H_{eq}. Typical values of H

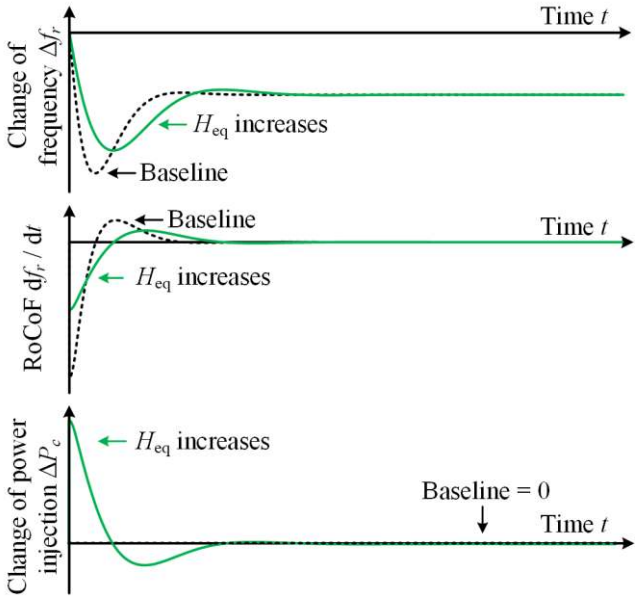

Fig. 4. Effect of equivalent inertia constant H_{eq}.

are found to be 5 s for gas-fired generators, 3.5 s for coal-fired generators, 4 s for nuclear generators, and 3 s for hydraulic generators [9], [25].

As the penetration levels of RESs grow, SGs are gradually being phased out by renewable generators. However, renewable generators are essentially power electronic converters without any direct inertia contribution. In consequence, RoCoF levels may become excessively high. This issue has already challenged the control and stability of small-scale power systems and will soon be faced by larger interconnected power systems.

One straightforward solution to the RoCoF concern is enhancing the RoCoF capabilities of generators, including both conventional and renewable generators. Many power system operators put more stringent requirements on RoCoF withstand capabilities through their rule change proposals to prevent generation tripping during frequency events [4], [6], [26], as formulated in Table II. According to the Ireland/North Ireland operators, compliance with the new RoCoF requirements would be the most efficient and timely solution to high-RoCoF issues [26]. However, high costs present a large obstacle that has retarded the adoption of stringent RoCoF standards by other power systems. A leading factor contributing to high costs is the RoCoF testing of generators (U.S. $1.5M per CCGT estimated by GE [8]). Obviously, it is unlikely to completely address the RoCoF concern by means of standard modifications, because this solution cannot mitigate RoCoF levels.

III. Proven Techniques for Inertia Enhancement

For clarity, this paper categorizes inertia enhancement techniques into two groups, i.e., the proven techniques that are already used in practice and the emerging techniques with active research efforts under way. More details will be disclosed next.

TABLE II
RULE CHANGES ON REQUIREMENTS OF ROCOF WITHSTAND CAPABILITIES FOR DIFFERENT COUNTRIES

Country/ region	Australia [4]	Great Britain [6]	Ireland/North Ireland [26]
Current requirement	Automatic access standard: ±4 Hz/s for 0.25 s, minimum access standard: ±1 Hz/s for 1 s	0.125 Hz/s for 0.5 s	0.5 Hz/s for 0.5 s
Future requirement	Non-synchronous systems: ±4 Hz/s for 0.25 s & ±3 Hz/s for 1 s Synchronous systems: automatic access standard: ±4 Hz/s for 0.25 s & ±3 Hz/s for 1 s, minimum access standard: ±1 Hz/s for 1 s	New synchronous units and non-synchronous units: 1 Hz/s for 0.5 s Incumbent synchronous units: 0.5 Hz/s for 0.5 s	1 Hz/s for 0.5 s

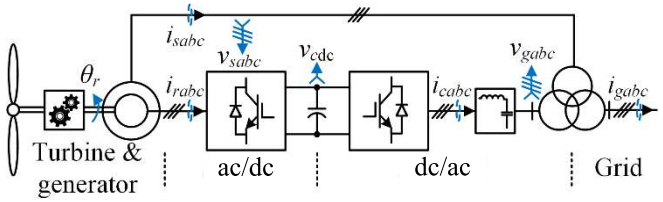

Fig. 5. Schematic of DFIG-based wind generation systems.

A. Inertia Enhancement by Synchronous Condensers

Synchronous condensers are essentially SGs running without prime movers or loads [9]. Normally, they are used for reactive power compensation and voltage control. Apart from this, synchronous condensers may also be employed to reap the benefit of their inertia. It has been reported that the typical value of H for synchronous condensers is 2.1 s [25]. In addition, synchronous condensers may be modified to improve their inertia contributions by adding additional rotating masses. Although the adoption of synchronous condensers eases the RoCoF issue, high capital and operating costs have deterred their widespread applications for inertia enhancement.

B. Inertia Emulation/Frequency Support by Wind Turbines

The wind energy has been regarded as one of the most promising RESs, and the inertia emulated by wind turbines provides added incentives for the use of wind energy. For wind generation system configurations, doubly fed induction generators (DFIGs) with partial-scale power converters are dominating on the market by far [27]–[29]. Fig. 5 illustrates a schematic of DFIG-based wind generation systems, where the stator of the DFIG is directly connected to the grid while the rotor is tied to the grid through a back-to-back converter consisting of a grid-side converter and a generator-side converter. The grid-side converter is intended to regulate the dc-link voltage and reactive power. In contrast, the generator-side converter seeks to control the active power and rotor speed, and it may also be used to regulate the reactive

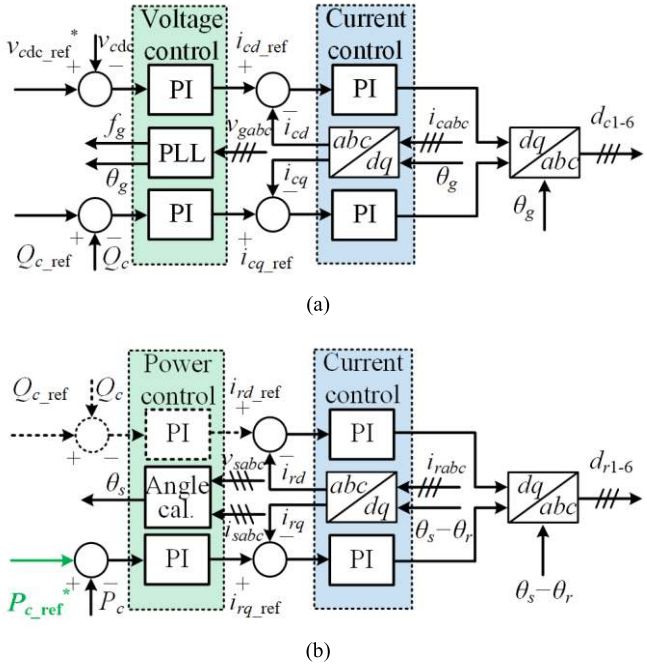

Fig. 6. Control architecture of DFIG-based wind turbine systems. (a) Control structure of grid-side converter. (b) Control structure of generator-side converter.

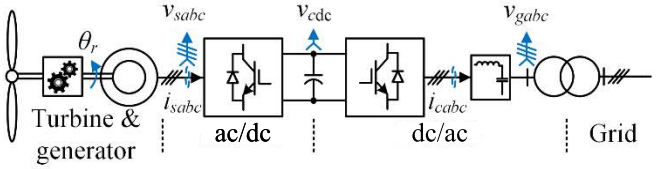

Fig. 7. Schematic of PMSG-based wind generation systems.

power. The relevant control architecture is detailed in Fig. 6, where the subscript ref denotes the reference notation, PI and PLL are the abbreviations of proportional-integral controller and phase-locked loop, f_g and θ_g are the frequency and phase angle estimated by the PLL, and P_c and Q_c are the active and reactive power injections calculated from signal measurements, respectively [30]. As shown in Fig. 6(b), the grid-injected power P_c can easily be regulated by modifying its reference $P_{c\_ref}^*$. Note that the decoupling terms between d- and q-axes are omitted and can be found in [31] and [32].

The trend of using SGs with full-scale power converters is appearing [27]–[29]. For demonstration, Fig. 7 illustrates a schematic of permanent magnet SG (PMSG)-based wind generation systems. As noticed, a back-to-back converter interconnects the stator windings of the wind turbine to the power grid. Although this solution necessitates high-power converters, it allows the elimination of slip rings, simplified or even eliminated gearbox, and enhanced power and speed controllability [27]. Its control architecture is illustrated in Fig. 8, where the d-axis current reference of the generator-side converter i_{sd_ref} is a function of the rotor angle θ_r for minimizing power losses. It should be recognized that the inertia emulation by DFIG- and PMSG-based wind

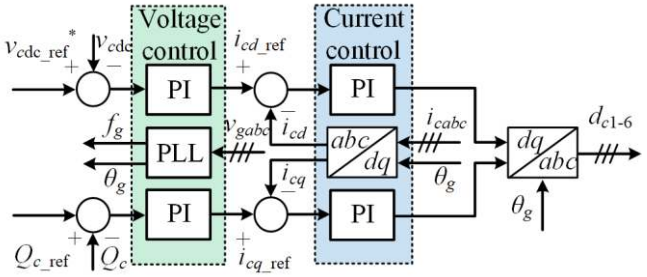

Fig. 8. Control architecture of PMSG-based wind turbine systems. (a) Control structure of grid-side converter. (b) Control structure of generator-side converter.

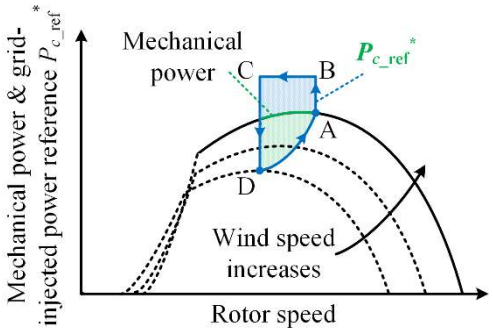

Fig. 9. Operating trajectory of a wind turbine during an under-frequency event.

turbines are both achieved by changing the grid-injected power P_c or the electromagnetic torque T_c.

To date, Hydro-Quebec and Ontario in Canada have mandated wind turbines for the delivery of inertial responses [8]. Fig. 9 presents the normal operating trajectory of a wind turbine during an under-frequency event. Initially, it is assumed that the wind turbine stays at the maximum power point A. Upon detecting a frequency event, the wind turbine increases the reference of the grid-injected power $P_{c\_ref}^*$ and registers its capability in boosting 5%–10% of its rated power within 1–2 s, and thus, the grid-injected power moves up to point B. The wind turbine maintains such a high-power injection for about 10 s until it reaches point C. In this process, the rotor slows down, because the input mechanical power of the wind turbine is less than its output power. After that, the turbine decreases its output power to point D (as much as a 30% reduction), and then, the rotor speed starts to recover due to the reduced output power until the turbine reaches point A (duration time up to 40 s) [8].

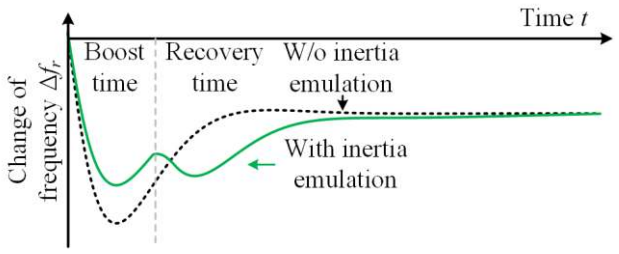

Fig. 10. Frequency response curves with/without inertia emulation by wind turbines.

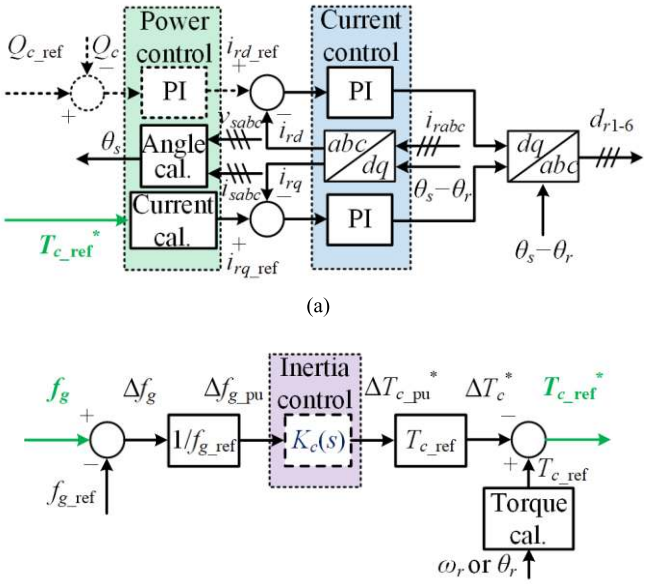

Fig. 11. Control architecture of wind turbines for inertia emulation. (a) Control structure of generator-side converter. (b) Control structure for inertia emulation.

Fig. 10 shows the corresponding frequency response curves. As evidenced, the inertia contributed by the wind turbine is different from the synchronous inertia. This can be understandable, as the wind turbine does not output the power exactly the same as SGs do during the frequency event (see Fig. 4). In this sense, the term "inertia emulation" may more precisely be replaced by "frequency support." In practice, grid codes normally specify the performance metrics including the minimum boost time, boost power, maximum actuation time, drop power, recovery time, and dead band [8].

To make the inertial responses of wind turbines more similarly as those of SGs, extensive research has been carried out. The idea of inertia emulation by wind turbines is proposed in [33] and [34], where the electromagnetic torque of DFIG-based wind turbines is regulated. Referring to Fig. 11(a), one can notice that the torque reference $T_{c\_ref}^*$ appears in the control structure of the generator-side converter instead of the power reference $P_{c\_ref}^*$ in Fig. 6(b). Fig. 11(b) details the supplementary control scheme for inertia emulation, where $K_c(s)$ is implemented as a differential controller, linking proportionally the RoCoF to the change in the torque reference ΔT_c^* [33]. It is further reported in [35] that the

emulated inertia can be expected from wind turbines even without the supplementary inertia control if the torque T_c is controlled slowly enough. However, this is achieved at the expense of torque tracking performances. Alternatively, it is recommended to implement $K_c(s)$ as a high-pass filter instead of a differential controller to avoid high-frequency noise amplification [34], [36]. However, in [34]–[36], the emulated inertia and synchronous inertia are still not identical. More importantly, the influence of inertia emulation on the aerodynamics of wind turbines and speed recovery processes are ignored in [33]–[36].

As pointed out by [37], speed recovery processes will greatly change the inertial responses of wind turbines and may even cause the rotor stall and system instability. To avoid the potential instability issue due to the speed recovery, Conroy and Watson [38] proposed to saturate the power outputs of wind turbines and recover their rotor speeds individually and sequentially. However, the proposed schemes make inertia control highly nonlinear. In another attempt, the key factors that determine the inertia emulation have been identified, including torque/power control modes, current saturations, compensator parameters, and inertial response shapes [39]. Moreover, it is revealed that the maximum power point tracking (MPPT) controller in wind turbines facilitates the speed recovery but deteriorates the effect of inertia emulation [39]. As such, the inertia emulation effect reduces to be similar as that shown in Fig. 10. The adoption of energy storage can resolve the concern introduced by the speed recovery and uncertain wind speeds [40], [41]. In addition, novel speed recovery strategies for better inertia emulation are still under active research [42], [43].

When wind speeds exceed their rated values, the additional power required by inertia emulation comes from wind instead of rotors by overloading wind turbines for a short period. In this case, wind turbines should be regulated through the pitch or active stall control, and therefore, speed recovery processes are no longer necessary [28], [32]. Note that, although inertial responses have been made practical by mandatory requirements rather than economic incentives in Hydro-Quebec, new opportunities for paying back such a service remain possible elsewhere. It is desirable to incorporate this function into new wind plants during the design and commission stage. Otherwise, retrofitting could be considerably more expensive.

IV. Emerging Techniques in Inertia Emulation

As the progress along the trajectory of renewable integration continues, there will be a growing penetration of emerging and evolving inertia enhancement techniques into the market. On the one hand, these techniques will create new opportunities for service providers to actively participate in the market. On the other hand, the recognition of these opportunities will enable system operators to improve the stability and reliability of future more-electronics power systems.

A. Inertia Emulation by Various Energy Storage Units

In order to emulate inertia, energy storage units should be employed and properly regulated to release or absorb energy in the same way as the rotors of SGs do. In this section, the emerging inertia emulation techniques are classified according to their energy storage units. Note that, the candidates of energy storage for frequency control include pumped hydro, compressed air, superconducting magnetic, fuel cell, capacitor, ultracapacitor, flywheel, and battery [44]–[46]. For inertia emulation, the uses of dc-link capacitors, ultracapacitors, and batteries have been reported and covered in this section.

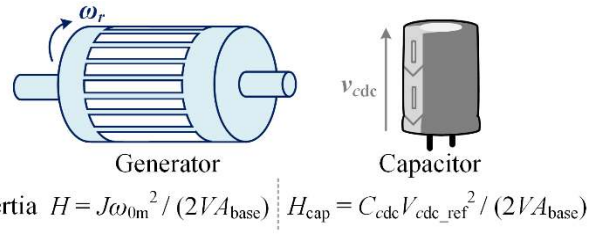

Fig. 12. Mapping between SGs and dc-link capacitors [48].

1) dc-Link Capacitors: dc-link capacitors are inherently necessary in nearly all types of grid-connected power converters for dc-link voltage support, harmonic filtering, and reactive power compensation [18]–[21], [47]. Recently, these capacitors are also showing great premise for relaxing the stresses due to high-RoCoF levels and low-frequency nadir through inertia emulation [48]–[51]. The mechanism for inertia emulation can well be explained by the mapping between SGs and dc-link capacitors, as shown in Fig. 12, where H_{cap} denotes the inertia constant of capacitors. From Fig. 12, the similarities between generators and capacitors can clearly be identified. Specifically, the dc-link voltage v_{cdc} (V_{cdc_ref} denotes its rated value) and capacitance C_{cdc} play similar roles as the frequency ω_r (f_r) and moment of inertia J, respectively.

This interesting observation results in the proposal of one simple frequency controller, which proportionally relates the grid frequency to the dc-link voltages of grid-connected power converters for generating the emulated inertia or known as the virtual inertia [48]–[51]. For illustration, the relevant system schematic and control architecture are detailed in Figs. 13 and 14, respectively [48]. Note that, the inductor filters, denoted by L_c in Fig. 13, can be replaced by higher-order passive filters to achieve better harmonic filtering and cost saving, as described in [52] and [53]. In Fig. 14(b), given that $K_c(s) = K_c$, the total inertia constant will approximately be changed from H_{eq} into $(H_{eq} + K_c H_{cap})$ after taking the effect of inertia emulation into consideration, and $(K_c H_{cap})$ represents the virtual inertia constant. The detailed derivation process of the virtual inertia constant can be found in [48].

The candidate applications of grid-connected power converters include wind generation (e.g., in Fig. 5), solar photovoltaic (PV) generation [54], energy storage systems (ESSs) [55]–[57], active power filters [58], static VAR compensators (STATCOMs) [59], variable speed drives [29], high-voltage direct current (HVdc) transmissions [60], and power supplies for data centers [61]. With regards to the HVdc application, modular multilevel converters (MMCs) are emerging as a pre-

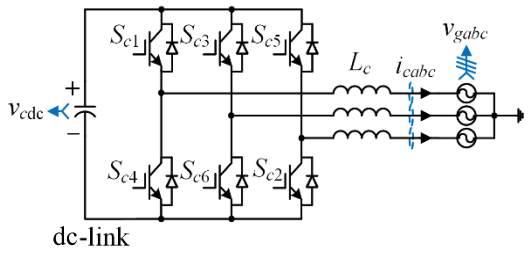

Fig. 13. Schematic of grid-connected power converters.

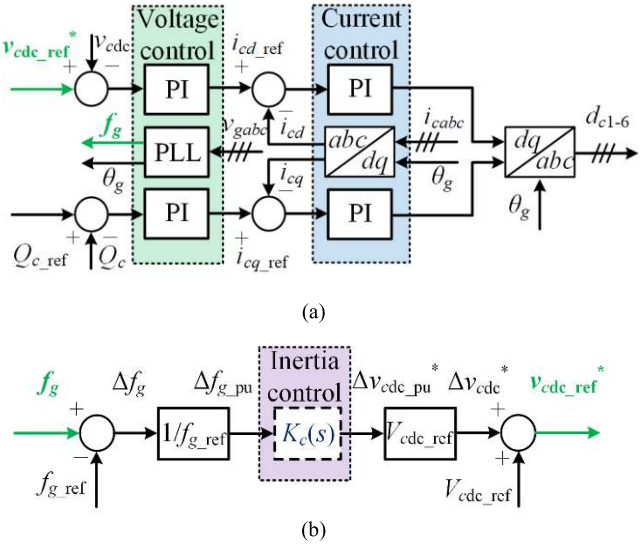

Fig. 14. Control architecture of grid-connected power converters for inertia emulation. (a) Basic control structure. (b) Control structure for inertia emulation.

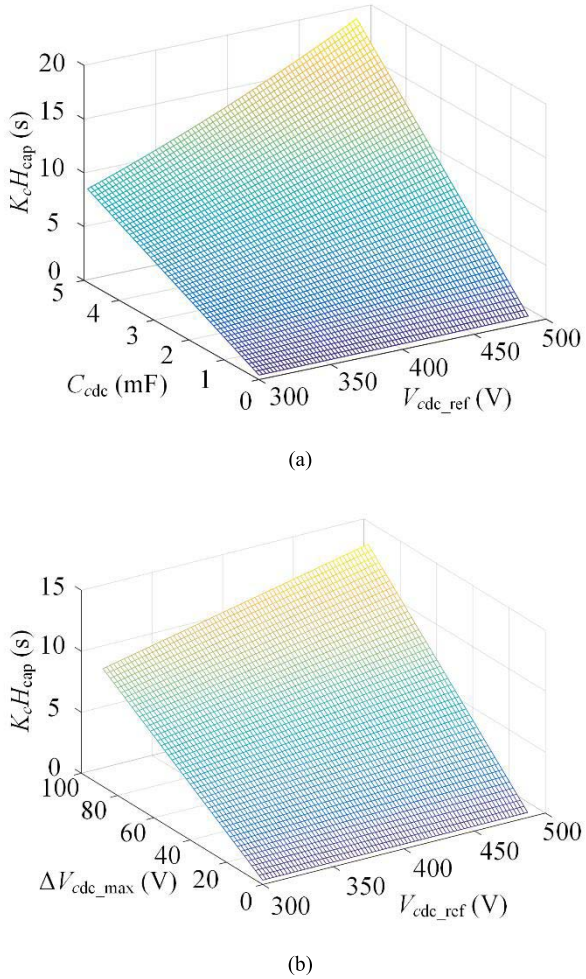

Fig. 15. Virtual inertia constant K_cH_{cap} versus C_{cdc}, V_{cdc_ref}, and ΔV_{cdc_max} ($\Delta f_{r\_max} = 0.2$ Hz, $f_{ref} = 50$ Hz, and $VA_{base} = 1$ kVA) [48]. (a) $\Delta V_{cdc\_max}/V_{cdc\_ref} = 0.15$. (b) $C_{cdc} = 2.82$ mF.

ferred topology [60]. Although capacitors may not explicitly be found in the dc bus of MMCs, they are distributed in the dc-link of each cell. Such capacitors collectively have a great potential for inertia emulation, as discussed in [62].

It is found that the virtual inertia constant (K_cH_{cap}) would be constrained by the dc-link capacitance C_{cdc}, rated voltage V_{cdc_ref}, and maximum allowable voltage change ΔV_{cdc_max}, as verified by Fig. 15 [48]. Among these parameters, ΔV_{cdc_max} may further be improved by injecting third-harmonic terms into modulating references [63].

To experimentally validate the effectiveness of emerging techniques in inertia emulation and improvement, a stand-alone more-electronics power system has been constructed and used as the test system. Fig. 16 illustrates a schematic of the test system, which consists of a virtual synchronous machine (VSM), a PV generation system, and an ESS. The VSM is employed here to regulate the grid frequency and provide the grid voltages in a similar way as conventional SGs do so that the inertia improvement can be validated. The designs of VSMs are detailed in [64] and [65]. The dc-links of the interfaced-power converters for the VSM, PV generation, and ESS can flexibly be connected to various components or circuits, e.g., capacitors, ultracapacitors, or dc–dc converters, depending on specific applications. Fig. 17 presents a photograph of the test system, where the dSPACE controller (Microlabbox) serves to control all the power converters.

The system and control parameters with regards to the experiments on the inertia emulation by dc-link capacitors can be found in [48], where the designed virtual inertia constant (K_cH_{cap}) is identical to the synchronous inertia constant H, i.e., $K_cH_{cap} = H = 5.0$ s. To visualize the effect of inertia emulation, Fig. 18 presents the experimental results of the power systems without and with the virtual inertia under a 3% step-up load change, where clear performance benefits in terms of RoCoF and frequency nadir can be identified. Specifically, the frequency nadir is improved 18% from 49.83 to 49.86 Hz; meanwhile, a 50% improvement of the RoCoF from -0.150 to -0.075 Hz/s can be expected. In the face of the frequency decline, power converters rapidly inject active power into the grid for inertia emulation, which improves the frequency control and may prevent grid collapses. In Fig. 18(b), ΔE_{c_pu} refers to the per unit output energy of power converters during the frequency event. Mathematically, ΔE_{c_pu} equals the per unit electrical energy released by the dc-link capacitors, i.e., $\Delta E_{c\_pu} = (0.5C_{cdc}V_{cdc\_ref}^2 - 0.5C_{cdc}v_{cdc}^2)/VA_{base}$, which is

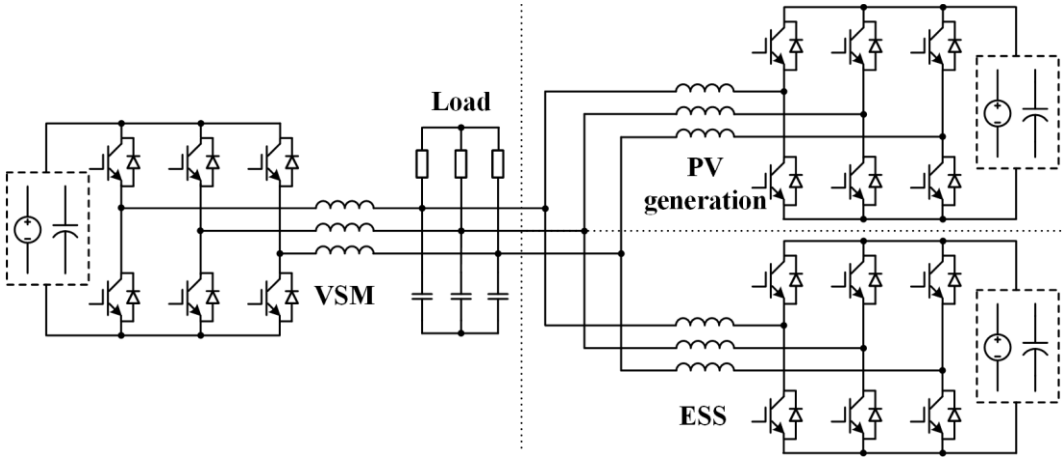

Fig. 16. Schematic of the test system.

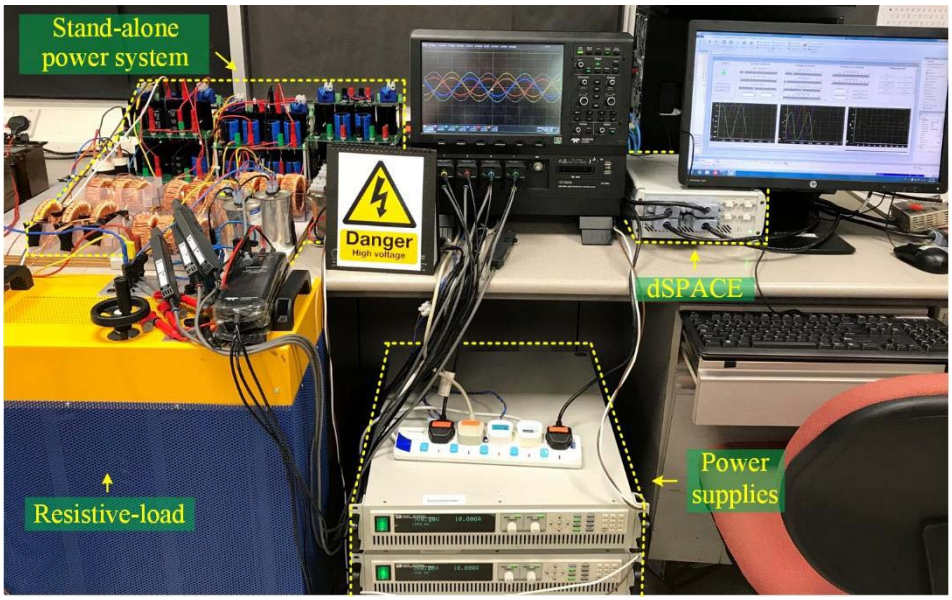

Fig. 17. Photograph of the test system.

also equivalent to the time integral of the per unit converter output power ΔP_{c_pu}.

It should be mentioned that power converters only generate the virtual inertia and help frequency control rather than providing the grid frequency in this case. In addition, unlike power electronic systems where 100% load step changes may occur, the step changes in power systems are mainly caused by the loss of generators or load shedding, and a 3%–5% load change is considered to be a large disturbance to power systems [9].

2) Ultracapacitors: When the inertia emulated by dc-link capacitors is insufficient and/or other frequency support functions are required, ESSs can further be employed. In ESSs, power converters serve as the interface between power grid and energy storage units and can provide a tight control of their charging states. The ESS topologies are summarized in [55]–[57]. Among the candidates of energy storage units in ESSs, ultracapacitors have the benefits of high-power density and long lifetime. Fig. 19 shows the schematic of a typical ultracapacitor storage system, where v_{uc} denotes the voltage across the ultracapacitor. Through a dc–dc converter, v_{uc} can be boosted into a higher dc-link voltage v_{cdc}, making possible the exploitation of a conventional two-level three-phase inverter for grid synchronization.

The basic control structures of ultracapacitor storage systems are represented by Fig. 20(a) and (b), where the PI controllers can be tuned according to the guidelines given in [66], and the voltage feed-forward and decoupling terms between d- and q-axes are not shown here for simplicity. After being properly designed, the dc–dc controller should enable the ultracapacitor voltage v_{uc} to accurately track its reference $v^*_{uc\_ref}$. Furthermore, to perform inertia emulation, a specific control scheme that directly relates the frequency to the ultracapacitor voltage is employed, as detailed in Fig. 20(c), whose principle is identical to that of Fig. 14(b). As compared with dc-link capacitors, ultracapacitors feature larger capacitances, hence, higher capabilities for inertia emulation. Moreover, the additional dc–dc converter can decouple the ultracapacitor from

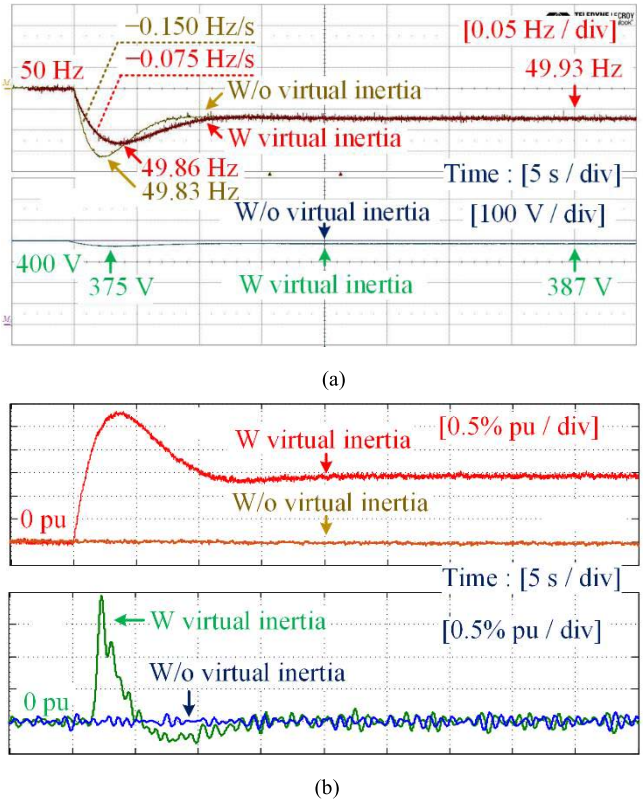

Fig. 18. Experimental results of power systems with and without the emulated inertia by dc-link capacitors under a 3% step-up load change [48]. (a) Frequency f_r (top) and dc-link voltage v_{cdc} (bottom). (b) Output energy ΔE_{c_pu} (top) and power ΔP_{c_pu} (bottom).

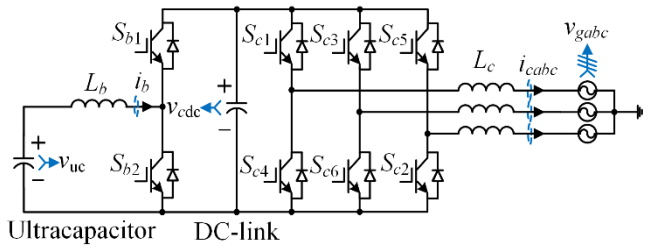

Fig. 19. Schematic of ultracapacitor storage systems.

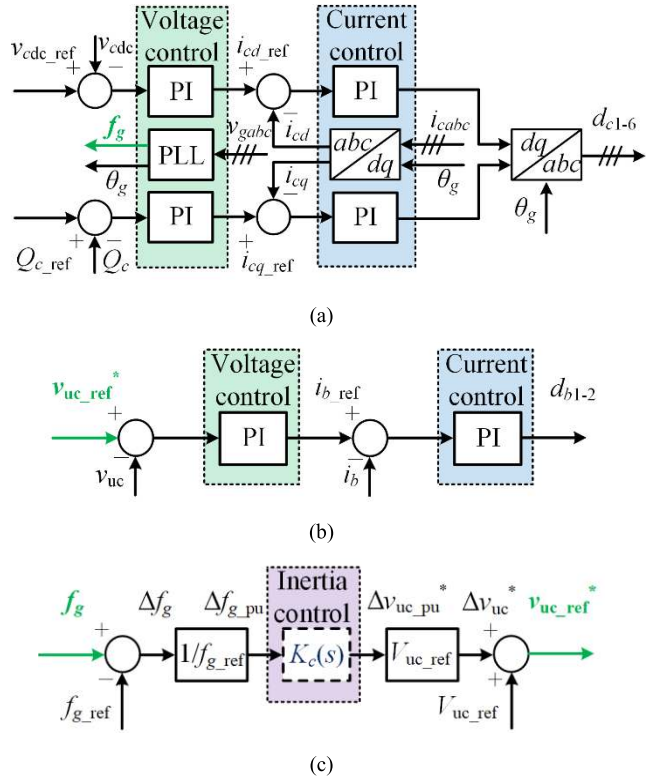

Fig. 20. Control architecture of ultracapacitor storage systems with inertia emulation. (a) Control structure of inverter. (b) Control structure of dc–dc converter. (c) Control structure for inertia emulation.

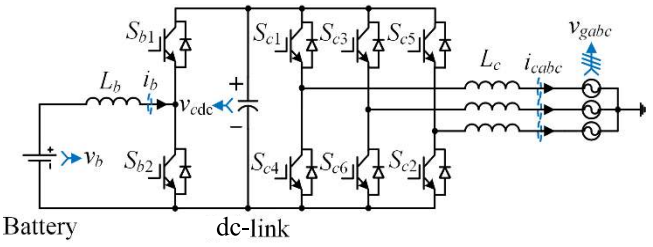

Fig. 21. Schematic of battery storage systems.

the dc-link, thus allowing a wider range of voltage variations and further inertia enhancement. The continued progress in ultracapacitors will make this technique more economically attractive.

3) Batteries: Characteristics such as high energy density, fast response, and moderate cost make batteries stand out among all the energy storage units when applied to frequency control. For instance, National Grid has defined the enhanced frequency response control scheme, which requires suppliers to respond fast to under-frequency events via the droop control within 1 s and sustain their outputs for at least 15 min, and tender results indicate that all the successful bidders are from battery storage providers (with a combined capacity of 201 MW) [67]. There are many attempts that use batteries for the droop control, e.g., in Hawaii [8]. In addition, the European Commission backed project "Twenties" contains several demonstrations concerning virtual power plants and frequency control by battery storage (i.e., Twenties demo 2), and these demonstrations were conducted to facilitate the integration of wind energy [68], [69].

Although batteries being used to emulate inertia have so far not been reported in the industry, this technique has a great potential for providing a degree of inertia control in the future. However, unlike capacitors or ultracapacitors, batteries feature almost fixed voltages in normal charging states, which cannot easily be regulated for inertia emulation. Alternatively, it is possible to tightly regulate the battery output power. Referring back to Fig. 3, the inertia constant H_{eq} can be increased to $(H_{\text{eq}} + K_c)$ if $K_c(s)$ is designed to be $2K_c s$. Therefore, for battery storage systems in Fig. 21, one possible implementation of inertia emulation is achieved by proportionally linking the active power reference and the RoCoF. The relevant control architecture of battery storage systems is detailed in Fig. 22, where the battery power P_c is

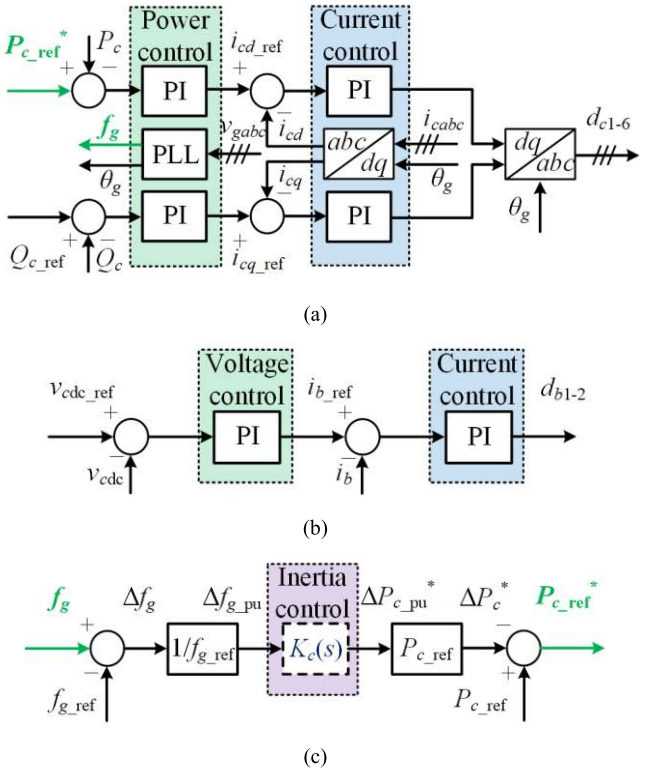

Fig. 22. Control architecture of battery storage systems with inertia emulation. (a) Control structure of inverter. (b) Control structure of dc–dc converter. (c) Control structure for inertia emulation.

regulated by the inverter controller. Moreover, $K_c(s)$ shown in Fig. 22(c) should be designed as a differential controller for inertia emulation, which requires the detection of RoCoF signals [74]. Similar inertia emulation schemes have already been applied to wind turbines, as illustrated in Fig. 11.

Fast and accurate RoCoF measurements are quite essential for not only protection of generating units but also inertia emulation. Nevertheless, the analyses from the industry field in Ireland and Great Britain have revealed that reliable measurements of RoCoF levels, particularly over a very short period, would create a significant challenge [8]. This is because direct differentiating the frequency signal may cause noise amplifications.

Solutions to this challenge have been seriously pursued. As examples, Xin *et al.* [70], [71] presented several noise-insensitive implementations of digital differentiators. It has been shown that the second-order generalized integrator (SOGI) enables the accurate estimations of the input signal and its derivative or quadrature signal at a predefined frequency. This feature may further be exploited to form the so-called frequency-locked loop (FLL), as detailed in Fig. 23, where $v_{g\alpha}^*$ and $qv_{g\alpha}^*$ are the estimations of grid voltage $v_{g\alpha}$ and its quadrature signal at frequency ω_g, respectively, and ω_g denotes the frequency estimated by the FLL [72]. From the input of the integrator (I) shown in Fig. 23(a), the RoCoF signal can be obtained.

The overall structure of FLLs follows that of PLLs [72]. However, heightened attention should be attached to the integrator shown in Fig. 23(a), which ensures a fast and

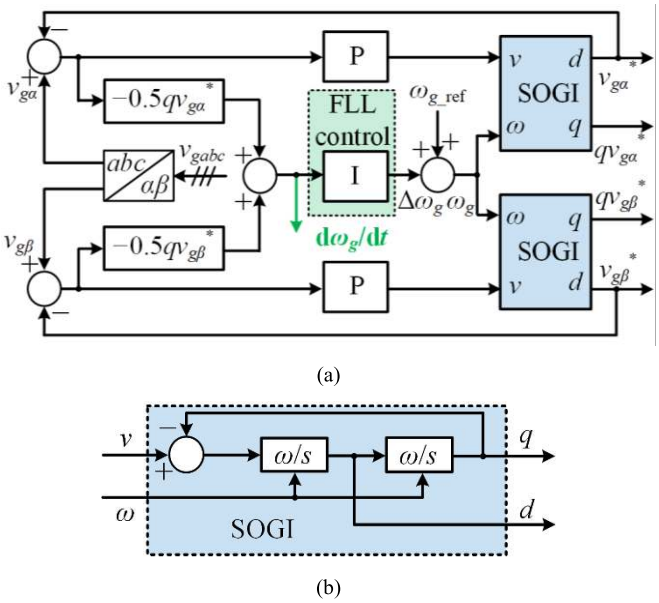

Fig. 23. Control architecture of three-phase FLLs [74]. (a) Overall structure. (b) Structure of SOGI.

accurate measurement of the RoCoF. Rather than integrators, PI controllers are normally used in PLLs; otherwise, the PLL control will become unstable. As a result, it would be difficult to estimate RoCoF signals by using PLLs. As compared with PLLs, FLLs feature better stability and robustness as they only estimate the frequency instead of both frequency and phase angle. Design guidelines for various FLLs can be found in [73], where it is reported that three-phase FLLs can remove the double-line-frequency ripples introduced by single-phase FLLs.

The system and control parameters related to the inertia emulation by batteries using FLLs are given in [74]. Fig. 24 demonstrates the effect of inertia emulation, where the emulated inertia improves the frequency nadir from 49.73 to 49.77 Hz (indicating a 15% improvement) and the RoCoF from −0.250 to −0.125 Hz/s (namely, a 50% improvement), respectively. Such improvements of frequency nadir and RoCoF validate the effectiveness of inertia emulation and RoCoF detection. In addition to FLLs, other methods for RoCoF detection are still under active research, and further developments in this direction will set the stage for the technique of inertia emulation through batteries. Duchwitz and Fischer [75] pointed out the potential instability issue faced by grid-connected power converters for inertia emulation by battery storage. It is concluded that a slow virtual inertia control can address the instability concern. The relevant analysis and conclusion are of importance and can provide useful guidelines for the virtual inertia design.

B. Frequency Control by Virtual Synchronous Machines

Presently, the objectives of grid frequency provision and regulation are mainly achieved by SGs. As SGs being gradually replaced by power electronics-interfaced renewable generators, power converters are supposed to form and regulate the grid frequency. Fortunately, the concept of

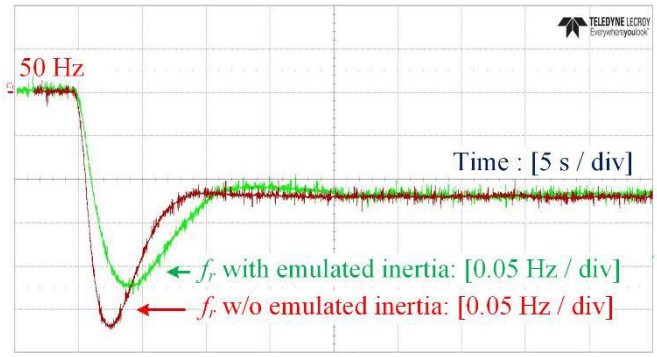

(a)

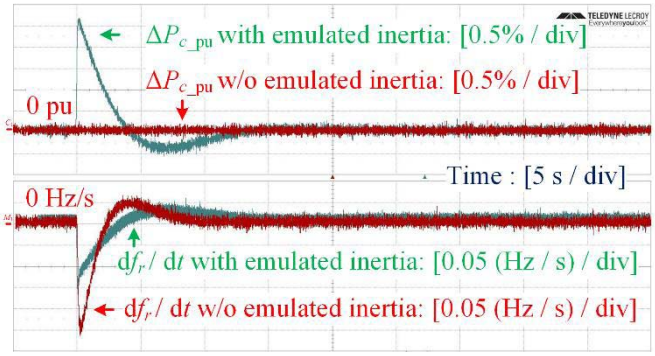

(b)

Fig. 24. Experimental results of power systems with and without the emulated inertia by a battery storage system under a 5% step-up load change. (a) Frequency f_r.(b) Output power ΔP_{c_pu} and RoCoF df_r/dt.

VSMs, i.e., VISMAs or virtual SGs (VSGs) has been proposed [76], [77]. It is reported that VSMs are essentially power converters emulating the operation of SGs, providing not only the power system inertia but also grid forming functions [76]–[78]. This section aims to review the implementations of VSMs for frequency control.

Various VSM models and control schemes have been introduced [76]–[93]. First, the complete mathematical model of SGs covering both mechanical part and electrical part (including armature windings, field windings, and amortisseurs, i.e., damping circuits) is constructed to make VSMs operate in the same way as SGs do so that the well-established theories for conventional power systems can still be valid for more-electronics power systems in [76], where VSMs are implemented as current-controlled inverters. Furthermore, the same research group proposes to implement VSMs based on a simplified model including the major mechanical part (the swing equation) and electrical part (armature windings) [79]. The proposed VSMs are then tested under an islanded power system, where undesirable over voltages during system start-ups are avoided through a soft start scheme [80]. Other VSM models without amortisseurs have been employed in [78], [81], and [82] and evaluated in [83], where ac voltages are regulated in addition to ac currents. Focusing on frequency control, VSM models can further be simplified [84]–[87], [89]–[91], [93]. It is pointed out in [84] and [85] that the essential VSM control, i.e., the swing equation, is equivalent to the low-pass-filtered power droop control, and their similarities and

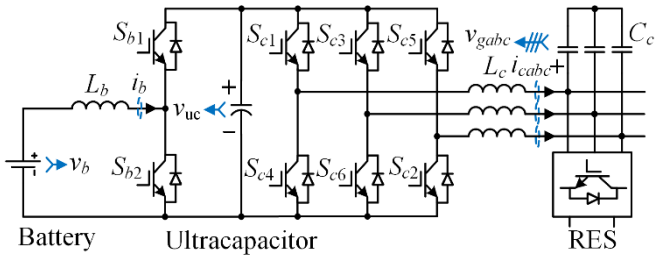

Fig. 25. Schematic of VSMs with hybrid energy storage systems.

differences are explored and evaluated in [86]. Furthermore, the VSM control schemes are reviewed and benchmarked in [85] and [93]. In this section, except for the swing equation, the speed governor and reheat turbine, which are collectively denoted by $K_g(s)$ in Fig. 3, are also employed in the VSM model. Note that, the concept of VSMs has been extended to HVdc transmissions and dc microgrids [94], [95].

One research direction refers to the energy storage used in VSMs for frequency control. Although dc-link capacitors seem to be one plausible choice, as suggested in [96]–[98] and Fig. 12, the frequency droop requires minute-to-hour-scale continuous power injections or absorptions, and capacitors (even ultracapacitors) are inadequate for this purpose due to their low energy density. Therefore, other energy storage units are necessary for VSMs. The battery storage deserves the credit for its high energy density, and therefore, it is suitable for the droop control [55], [65]. Moreover, the inertia emulation by battery storage is also feasible, as discussed in Section IV-A. Therefore, the battery storage can be used for frequency control in VSMs. However, the power required by inertia emulation is in proportional to the time derivative of the grid frequency, i.e., the RoCoF. In consequence, as the grid frequency varies, the battery will frequently be charged and discharged, leading to the reduced battery lifetime and system efficiency, which become the major drawback of using the battery storage alone. Note that, capacitors or ultracapacitors featuring a high power density allow fast charge and discharge [65]. Considering different attributes of batteries and capacitors, they can simultaneously be employed in VSMs, where batteries compensate the long-term power required by the droop control while capacitors/ultracapacitors tackle the short-term power for inertia emulation.

Fig. 25 visualizes one VSM implementation following this idea, where a hybrid ESS consisting of a battery and an ultracapacitor is connected in parallel with the RES generation system operated in the MPPT mode [65]. Similar to Fig. 21, the ultracapacitor is interposed between dc–dc converter and inverter. However, the VSM controls the ac voltages v_{gx} $(x = a, b, c)$ besides the ac currents i_{cx}. Note that, Fig. 25 is only one possible VSM implementation instead of the standard VSM architecture. Such a VSM implementation is to reduce the fluctuations and changing rates of battery power in order to extend the battery lifetime and system efficiency [65].

Fig. 26 presents the control architecture of VSMs. It should be highlighted that the models of swing equation, speed governor, and turbine have been included in the VSM control, where the outer frequency control loop can be found

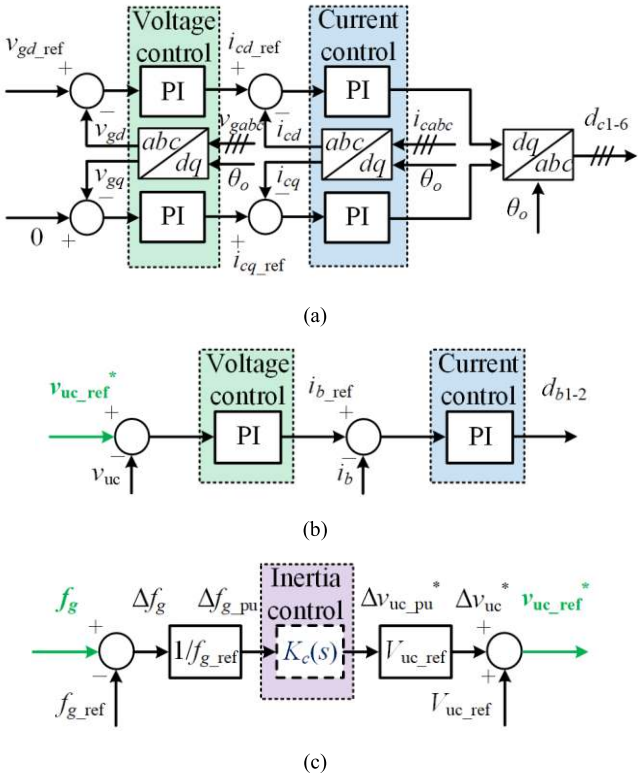

Fig. 26. Control architecture of VSMs. (a) Control structure of inverter. (b) Control structure of dc–dc converter. (c) Control structure for inertia emulation.

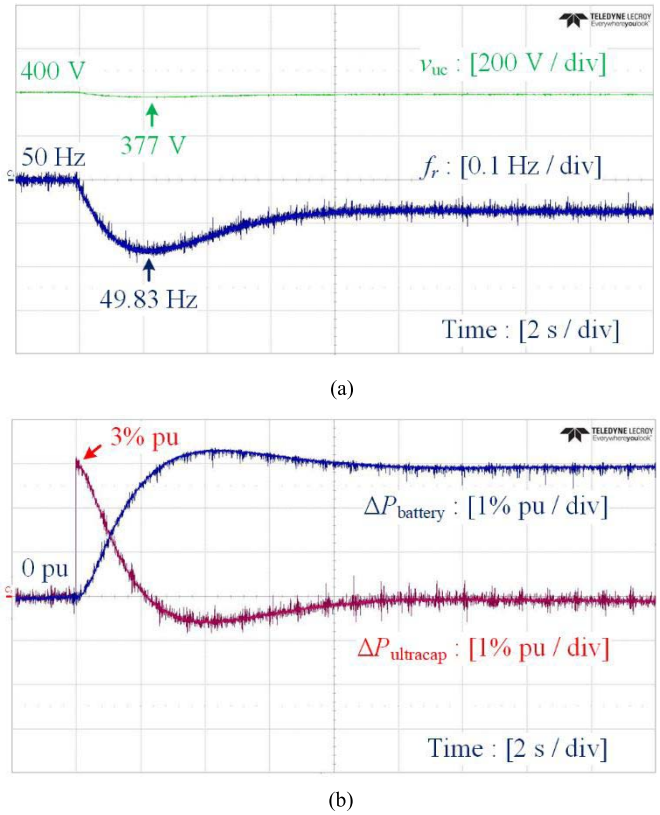

Fig. 27. Experimental results of the VSM under a 3% step-up load change [65]. (a) Ultracapacitor voltage v_{uc} and frequency f_r. (b) Battery power change $\Delta P_{battery}$ and ultracapacitor power change $\Delta P_{ultracap}$.

in Fig. 3 [65]. Note that, the phase angle θ_o in Fig. 26(a) is internally generated from the integral of the frequency signal Δf_{r_pu} in Fig. 3. Moreover, the grid frequency f_g is detected from a PLL in Fig. 26(c) for further allocating the VSM power into different energy storage units [65]. Specifically, the controller of the dc–dc converter regulates the dc-link voltage or the ultracapacitor voltage in proportion to the grid frequency to allocate the power required by inertia emulation into the ultracapacitor, and this control follows the principle of Fig. 14(b). In consequence, the battery sees and compensates only for long-term power fluctuations.

The system and control parameters concerning the frequency control by VSMs are presented in [65]. The experimental results of the VSM with hybrid energy storage under a 3% step-up load change are shown in Fig. 27. It should be mentioned that these experimental results focus on the power allocation between the energy storage units in the VSM rather than the improvement of frequency control. As noticed, the hybrid energy storage architecture allows the battery power to change slowly. Moreover, this power allocation method provides a clear guideline for energy storage sizing [65].

V. Other Technical Issues

A. Time Delays

Ideally, power converters should immediately output power following its references for frequency support. However, in practice, the time delays introduced by communications and converter control are inevitable, which will degrade frequency control and may even destabilize the entire power system [99], [100]. First, the time delays due to communications, e.g., the transport time delay from center control stations to individual power converters (up to several seconds), can be minimized through the decentralized control [101]. Specifically, the decentralized control establishes a rule for individual power converters to follow without communications, e.g., the frequency droop control. Through this approach, a global objective, e.g., the active power sharing, can automatically be achieved by all the participators. However, the tradeoff between the benefits introduced by the decentralized control and those due to the centralized control, e.g., the mitigation of RES variability, is required.

Second, the time delays associated with the power control of individual power converters may also be considerable. For instance, PV and wind generation systems can operate either in the conventional MPPT mode or in the constant power control mode. When frequency support is required, the transitions between MPPT mode and constant power mode become necessary, and such transitions or power control schemes introduce time delays. It should be commented that the dynamics of the presented inertia emulation schemes (Figs. 14, 20, 22, and 26) are much faster (less than a fraction of second) than those due to the mode transitions (up to several seconds), and such fast responses are sufficient for inertia support in a standard frequency regulation framework (Fig. 3). In addition, although the employment of energy storage allows PV and wind generations systems to work solely in the MPPT mode, this will bring in other concerns, e.g., high costs and

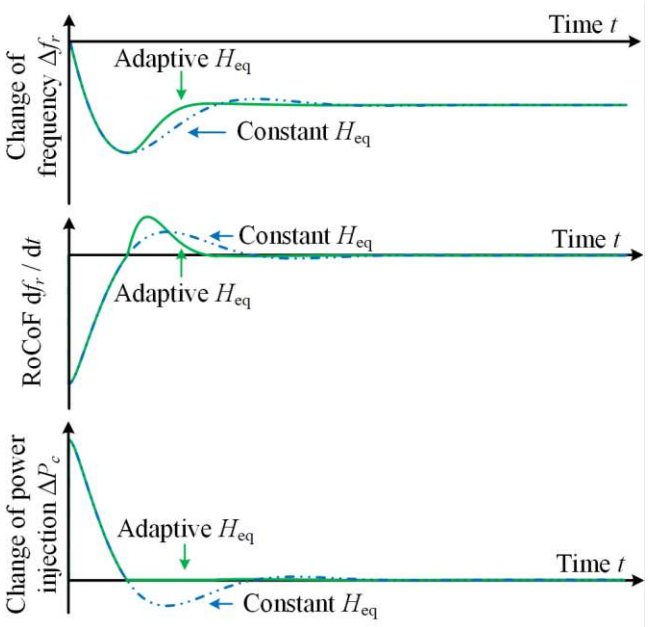

Fig. 28. Effect of an adaptive inertia control scheme.

limited lifecycle. Some power system operators, such as the California ISO, have already mandated the curtailment of PV plants at times, and hence, frequency support may be exercised without incurring any opportunity cost [99]. It remains to be a research direction for PV plants without energy storage to provide frequency support including inertia emulation, and the relevant time-delay issues require further investigations. Several schemes allowing fast and smooth power control have been developed in [99] and [102] and further summarized in [103]. Extensive research on time delays as well as their effects on the system stability is still on-going.

B. Adaptive Inertia

The fast-responding feature of power converters enables inertia suppliers to change their inertia contributions during frequency events, and hence, the further improvement of frequency control can be expected. For illustration, Fig. 28 visualizes the effect of a simple adaptive inertia control scheme. In this scheme, high inertia, i.e., large H_{eq}, is applied to support frequency control only before the frequency reaches its nadir. As a result, this method allows a faster frequency restoration as compared with the constant H_{eq} case. Similar adaptive inertia control schemes featuring fast frequency recovery and less oscillation have been reported in [104] and [105]. The fundamental principle behind these schemes is to emulate inertia when the frequency change Δf_r and RoCoF df_r/dt are of the same sign, and vice versa. A more advanced and complicated self-tuning algorithm has been proposed for minimizing the frequency deviation, RoCoF, and energy required by inertia emulation and damping in [106]. This algorithm searches continuously for the optimal inertia constant and damping constant during frequency events, thus reducing the energy yield for mitigating frequency disturbances. However, the nonlinear nature of adaptive inertia control may negatively influence the stability of power systems. This issue should be carefully investigated in future research.

C. Placement of Inertia

For large power systems, both the time-varying inertia profiles and locations of inertia may greatly influence the effectiveness of inertia emulation [107]. For the inertia emulation by energy storage units, e.g., ultracapacitors and batteries, one special issue is where to optimally place energy storage units. An optimization program has been developed to maximize the damping ratio of each power system mode so that the oscillations between generators can be minimized in [107]. Experiences drawn from [107] indicate that the high inertia at end notes can be more effective in suppression of oscillations. Rather than the damping ratio, an H_2 norm performance metric reflecting the network coherency has been proposed and optimized to determine the placements of inertia in [108]. It is reported that the H_2-norm-based optimal inertia allocation would be superior in terms of frequency overshoots and control efforts. These results may provide insightful guidance on the day-ahead planning of inertia. Note that, the fluctuations of inertia caused by RES variability and limitations of inertia suppliers must be considered before performing the day-ahead inertia scheduling.

D. Market Design for Inertia Service

A well-functioning market for the inertia service should clearly be designed before the emerging inertia emulation techniques can successfully be deployed. Currently, inertia is considered to be an inherent property in most power systems, thus being excluded from ancillary services markets. To design a market for the inertia service, inertia-related requirements on frequency control, such as RoCoF constraints, must be incorporated in the market clearing engine, and then, the inertia service should be co-optimized with other ancillary services. As an example, one market design explicitly incentivizing resources to provide the inertia support for the primary frequency control has been proposed in [109]. Moreover, the market design results of several case studies can be found in [110].

VI. Future Trend

The lack of inertia challenge has already been faced by small-scale power systems with relatively high levels of renewable penetration. As the trend of renewable integration continues, larger power systems will face similar issues soon [111]. To tackle the inertia issue, it is likely that more than one technique for inertia enhancement, as summarized in Table III, will simultaneously be employed to improve frequency control. In Table III, the column "Proven" refers to the proven techniques. Specifically, the proven techniques are the techniques that are already accepted and utilized in the industry. For example, the inertial responses from wind turbines have been mandated in Hydro-Quebec, Canada [8]. In contrast, the use of emerging techniques has so far not been reported in real commercial power systems. For instance,

TABLE III
SUMMARY OF INERTIA ENHANCEMENT TECHNIQUES

Inertia enhancement technique	Form of energy	Proven	Cost	Other function	Special concern
Synchronous condensers	Kinetic energy	✓	High	Reactive power compensation and voltage control	–
Wind turbines	Kinetic energy	✓	Low	Renewable integration	Nonlinear inertia emulation
DC-link capacitors	Electrical energy	×	Low	DC-link voltage support and harmonic filtering	Sizing of DC-link capacitors
Ultracapacitors	Electrical energy	×	High	Frequency control	Sizing and placement of ultracapacitors
Batteries	Electrochemical energy	×	High	Frequency control	RoCoF measurement, sizing and placement of batteries
VSMs	Source-dependent	×	High	Grid forming and frequency control	Sizing of energy storage

although the VSMs with hybrid energy storage have been experimentally verified, they are still not permitted to form the commercial power grid. Therefore, the VSM is concluded to be an emerging technique instead of a proven one.

As noted from Table III, although the adoption of synchronous condensers directly coupled to the grid is a well-proven technique, it only serves as a second choice for inertia enhancement due to high costs. The inertia coming from wind turbines has already demonstrated its cost effectiveness in practice and will enjoy a growing popularity in the future. Presently, the inertia emulated by wind turbines is still different from the synchronous inertia, and advances in the turbine control will make it identical to the synchronous inertia and even more attractive in the future [40]–[43].

Heightened attention should be paid to the technique of the inertia emulation by dc-link capacitors. It is supposed to greatly improve frequency control in an easy way with the minimized or even no hardware change. The optimization of dc-link capacitances with the goal of minimizing the cost, RoCoF, and frequency nadir under the constraint of linear modulations will be another research direction in the future. For the cases where the inertia emulated by dc-link capacitors is insufficient, ultracapacitors featuring higher capacitances can be employed as an alternative. The fast and accurate measurement of RoCoF signals is a challenge, slowing the practice of the inertia emulation by batteries. After the concern being addressed, this technique will become a promising solution to high-RoCoF levels.

Along with the increasing use of power electronics, power systems will be gradually transitioning toward power electronics-dominated power systems, where most of generators and loads are coupled to the grid via power electronics [112]–[115]. Under these scenarios, VSMs are expected to be the enabling components for grid forming and frequency control, and the role of inertia provision will transform from SGs to VSMs. Remember that not all the power converters in such power systems are allowed operating as current-controlled or grid-feeding converters [112]. In addition, since VSMs allow a much faster power balance and real-time tuning of control parameters as compared with SGs, the future inertia demand may become entirely different.

VII. CONCLUSION

This paper has presented a comprehensive review of inertia enhancement techniques allowing the improvements of frequency nadir and RoCoF in future more-electronics power systems. Among these techniques, the inertia emulation by wind turbines has already demonstrated its cost effectiveness in practice and will be pursued by more power system operators. Although being proposed recently, the concept of the inertia emulation by dc-link capacitors featuring the minimized or even no hardware change shows great promise due to its low cost. As compared with dc-link capacitors, ultracapacitors have larger capacitances and higher flexibility for inertia emulation. In addition, batteries will become another important inertia supplier after the successful development of fast and accurate RoCoF measurement schemes. As the trend of renewable integration continues, VSMs will eventually serve as the enabling components for inertia provision and frequency control in replacement of SGs in the future.

ACKNOWLEDGMENT

The authors would like to thank the anonymous associate editor and reviewers for their valuable and constructive comments that greatly improve the quality of this paper.

REFERENCES

[1] *War of the Currents*. Accessed: Dec. 4, 2017. [Online]. Available: https://en.wikipedia.org/wiki/War_of_the_currents
[2] N. Tesla, *A New System of Alternate Current Motors and Transformers*. Piscataway, NJ, USA: American Institute of Electrical Engineers, 1888.
[3] A. C. Monteith and C. F. Wagner, *Electrical Transmission and Distribution Reference Book*, 4th ed. New York, NY, USA: Westinghouse Electric Corporation, 1950, p. 6.
[4] *Electricity Rule Change Proposal*, Aust. Energy Market Operator, Melbourne, VIC, Australia, 2017. [Online]. Available: http://www.aemo.com.au

[5] *Fast Frequency Response in the NEM*, Aust. Energy Market Operator, Melbourne, VIC, Australia, 2017. [Online]. Available: http://www.aemo.com.au

[6] *The Grid Code*, National Grid, London, U.K., 2017. [Online]. Available: http://www.nationalgrid.com

[7] *Enhancement to the Spinning Reserve Requirements for the Singapore Power System*, Energy Market Authority, Singapore, 2017. [Online]. Available: http://www.ema.gov.sg

[8] *International Review of Frequency Control Adaptation*, Aust. Energy Market Operator, Melbourne, VIC, Australia, 2017. [Online]. Available: http://www.aemo.com.au.

[9] P. Kundur, *Power System Stability and Control*. New York, NY, USA: McGraw-Hill, 1994.

[10] *Mains Electricity by Country*. Accessed: Nov. 19, 2017. [Online]. Available: https://en.wikipedia.org/wiki/Mains_electricity_by_country

[11] *The Frequency Operating Standard*, Aust. Energy Market Commission, Sydney, NSW, Australia, 2017. [Online]. Available: http://www.aemc.gov.au

[12] *Power Supply Business Regulation*, (in Chinese), Nation Energy Admin., Beijing, China, 2016. [Online]. Available: http://www.nea.gov.cn

[13] European Network of Transmission System Operators for Electricity, Brussels, Belgium, (2017). *P1–Policy 1: Load-Frequency Control and Performance*. [Online]. Available: http://www.entsoe.eu

[14] *Report on the Quality of Electricity Supply*, Org. Cross-Regional Coordination Transmiss. Operators, Tokyo, Japan, 2016. [Online]. Available: http://www.occto.or.jp

[15] *Reliability Standards for the Bulk Electric Systems of North America*, North Amer. Electr. Rel. Corp., North Tower, GA, USA, 2017. [Online]. Available: http://www.nerc.com.

[16] Y. G. Rebours, D. S. Kirschen, M. Trotignon, and S. Rossignol, "A survey of frequency and voltage control ancillary services—Part I: Technical features," *IEEE Trans. Power Syst.*, vol. 22, no. 1, pp. 350–357, Feb. 2007.

[17] F. Blaabjerg, R. Teodorescu, M. Liserre, and A. V. Timbus, "Overview of control and grid synchronization for distributed power generation systems," *IEEE Trans. Ind. Electron.*, vol. 53, no. 5, pp. 1398–1409, Oct. 2006.

[18] J. M. Carrasco *et al.*, "Power-electronic systems for the grid integration of renewable energy sources: A survey," *IEEE Trans. Ind. Electron.*, vol. 53, no. 4, pp. 1002–1016, Jun. 2006.

[19] F. Blaabjerg, Z. Chen, and S. B. Kjaer, "Power electronics as efficient interface in dispersed power generation systems," *IEEE Trans. Power Electron.*, vol. 19, no. 5, pp. 1184–1194, Sep. 2004.

[20] B. Singh, B. N. Singh, A. Chandra, K. Al-Haddad, A. Pandey, and D. P. Kothari, "A review of single-phase improved power quality AC-DC converters," *IEEE Trans. Ind. Electron.*, vol. 50, no. 5, pp. 962–981, Oct. 2003.

[21] B. Singh, B. N. Singh, A. Chandra, K. Al-Haddad, A. Pandey, and D. P. Kothari, "A review of three-phase improved power quality AC-DC converters," *IEEE Trans. Ind. Electron.*, vol. 51, no. 3, pp. 641–660, Jun. 2004.

[22] *RoCoF—An Independent Analysis on the Ability of Generators to Ride Through Rate of Change of Frequency Values up to 2 Hz/s*, EirGrid/SONI, London, U.K., Feb. 2013.

[23] *Smart Frequency Control Project—The Balance of Power*, Nat. Grid, London, U.K., 2017. [Online]. Available: http://www.nationalgridconnecting.com

[24] *Future Power System Security Program—Progress Report*, Aust. Energy Market Operator, Melbourne, VIC, Australia, 2016. [Online]. Available: http://www.aemo.com.au

[25] E. Spahic, D. Varma, G. Beck, G. Kuhn, and V. Hild, "Impact of reduced system inertia on stable power system operation and an overview of possible solutions," in *Proc. PESGM*, Boston, MA, USA, Jul. 2016, pp. 1–5.

[26] *RoCoF Modification Proposal—TSOs' Recommendations*, EirGrid/SONI, Ballsbridge, Republic of Ireland, Sep. 2012.

[27] F. Blaabjerg and K. Ma, "Future on power electronics for wind turbine systems," *IEEE J. Emerg. Sel. Topics Power Electron.*, vol. 1, no. 3, pp. 139–152, Sep. 2013.

[28] Z. Chen, J. M. Guerrero, and F. Blaabjerg, "A review of the state of the art of power electronics for wind turbines," *IEEE Trans. Power Electron.*, vol. 24, no. 8, pp. 1859–1875, Aug. 2009.

[29] F. Blaabjerg, M. Liserre, and K. Ma, "Power electronics converters for wind turbine systems," *IEEE Trans. Ind. Appl.*, vol. 48, no. 2, pp. 708–719, Mar./Apr. 2012.

[30] H. Akagi, Y. Kanazawa, and A. Nabae, "Instantaneous reactive power compensators comprising switching devices without energy storage components," *IEEE Trans. Ind. Appl.*, vol. IA-20, no. 3, pp. 625–630, May/Jun. 1984.

[31] R. Pena, J. C. Clare, and G. M. Asher, "Doubly fed induction generator using back-to-back PWM converters and its application to variable-speed wind-energy generation," *IEE Proc.-Electr. Power Appl.*, vol. 143, no. 3, pp. 231–241, May 1996.

[32] S. Müller, M. Deicke, and R. W. De Doncker, "Doubly fed induction generator systems for wind turbines," *IEEE Ind. Appl. Mag.*, vol. 8, no. 3, pp. 26–33, May/Jun. 2002.

[33] L. Holdsworth, J. Ekanayake, and N. Jenkins, "Power system frequency response from fixed speed and doubly fed induction generator-based wind turbines," *Wind Energy*, vol. 7, no. 1, pp. 21–35, 2004.

[34] J. Ekanayake and N. Jenkins, "Comparison of the response of doubly fed and fixed-speed induction generator wind turbines to changes in network frequency," *IEEE Trans. Energy Convers.*, vol. 19, no. 4, pp. 800–802, Dec. 2004.

[35] A. Mullane and M. O'Malley, "The inertial response of induction-machine-based wind turbines," *IEEE Trans. Power Sys.*, vol. 20, no. 3, pp. 1496–1503, Aug. 2005.

[36] G. Lalor, A. Mullane, and M. O'Malley, "Frequency control and wind turbine technologies," *IEEE Trans. Power Sys.*, vol. 20, no. 4, pp. 1905–1913, Nov. 2005.

[37] J. Morren, S. W. H. de Haan, W. L. Kling, and J. A. Ferreira, "Wind turbines emulating inertia and supporting primary frequency control," *IEEE Trans. Power Syst.*, vol. 21, no. 1, pp. 433–434, Feb. 2006.

[38] J. F. Conroy and R. Watson, "Frequency response capability of full converter wind turbine generators in comparison to conventional generation," *IEEE Trans. Power Syst.*, vol. 23, no. 2, pp. 649–656, May 2008.

[39] M. Kayikçi and J. V. Milanovic, "Dynamic contribution of DFIG-based wind plants to system frequency disturbances," *IEEE Trans. Power Syst.*, vol. 24, no. 2, pp. 859–867, May 2009.

[40] M. F. M. Arani and E. F. El-Saadany, "Implementing virtual inertia in DFIG-based wind power generation," *IEEE Trans. Power Syst.*, vol. 28, no. 2, pp. 1373–1384, May 2013.

[41] L. Miao, J. Wen, H. Xie, C. Yue, and W. J. Lee, "Coordinated control strategy of wind turbine generator and energy storage equipment for frequency support," *IEEE Trans. Ind. Appl.*, vol. 51, no. 4, pp. 2732–2742, Jul. 2015.

[42] L. Ruttledge, N. W. Miller, J. O'Sullivan, and D. Flynn, "Frequency response of power systems with variable speed wind turbines," *IEEE Trans. Sustain. Energy*, vol. 3, no. 4, pp. 683–691, Oct. 2012.

[43] K. Liu, Y. Qu, H.-M. Kim, and H. Song, "Avoiding frequency second dip in power unreserved control during wind power rotational speed recovery," *IEEE Trans. Power Syst.*, vol. 33, no. 3, pp. 3097–3106, May 2018.

[44] P. F. Ribeiro, B. K. Johnson, M. L. Crow, A. Arsoy, and Y. Liu, "Energy storage systems for advanced power applications," *Proc. IEEE*, vol. 89, no. 12, pp. 1744–1756, Dec. 2001.

[45] G. Delille, B. Francois, and G. Malarange, "Dynamic frequency control support by energy storage to reduce the impact of wind and solar generation on isolated power system's inertia," *IEEE Trans. Sustain. Energy*, vol. 3, no. 4, pp. 931–939, Oct. 2012.

[46] H. Zhou, T. Bhattacharya, D. Tran, T. S. T. Siew, and A. M. Khambadkone, "Composite energy storage system involving battery and ultracapacitor with dynamic energy management in microgrid applications," *IEEE Trans. Power Electron.*, vol. 26, no. 3, pp. 923–930, Mar. 2011.

[47] H. Wang and F. Blaabjerg, "Reliability of capacitors for DC-link applications in power electronic converters—An Overview," *IEEE Trans. Ind. Appl.*, vol. 50, no. 5, pp. 3569–3578, Sep./Oct. 2014.

[48] J. Fang, H. Li, Y. Tang, and F. Blaabjerg, "Distributed power system virtual inertia implemented by grid-connected power converters," *IEEE Trans. Power Electron.*, vol. 33, no. 10, pp. 8488–8499, Oct. 2018.

[49] E. Waffenschmidt and R. S. Y. Hui, "Virtual inertia with PV inverters using DC-link capacitors," in *Proc. ECCE Eur.*, Karlsruhe, Gemany, Sep. 2016, pp. 1–10.

[50] J. Fang, X. Li, and Y. Tang, "Grid-connected power converters with distributed virtual power system inertia," in *Proc. IEEE Energy ECCE*, Cincinnati, OH, USA, Oct. 2017, pp. 4267–4273.

[51] E. Waffenschmidt, "Virtual inertia grid control with LED lamp driver," in *Proc. IESC*, Cologne, Germany, Jun./Jul. 2016, pp. 1–6.

[52] R. N. Beres, X. Wang, M. Liserre, F. Blaabjerg, and C. L. Bak, "A review of passive power filters for three-phase grid-connected voltage-source converters," *IEEE Trans. J. Emerg. Sel. Topics Power Electron.*, vol. 4, no. 1, pp. 54–69, Mar. 2016.

[53] J. Fang, X. Li, X. Yang, and Y. Tang, "An integrated trap-LCL filter with reduced current harmonics for grid-connected converters under weak grid conditions," *IEEE Trans. Power Electron.*, vol. 32, no. 11, pp. 8446–8457, Nov. 2017.

[54] S. B. Kjaer, J. K. Pedersen, and F. Blaabjerg, "A review of single-phase grid-connected inverters for photovoltaic modules," *IEEE Trans. Ind. Appl.*, vol. 41, no. 5, pp. 1292–1306, Sep./Oct. 2006.

[55] S. M. Lukic, J. Cao, R. C. Bansal, F. Rodriguez, and A. Emadi, "Energy storage systems for automotive applications," *IEEE Trans. Ind. Electron.*, vol. 55, no. 6, pp. 2258–2267, Jun. 2008.

[56] A. Khaligh and Z. Li, "Battery, ultracapacitor, fuel cell, and hybrid energy storage systems for electric, hybrid electric, fuel cell, and plug-in hybrid electric vehicles: State of the art," *IEEE Trans. Veh. Technol.*, vol. 59, no. 6, pp. 2806–2814, Jul. 2010.

[57] J. Cao and A. Emadi, "A new battery/ultracapacitor hybrid energy storage system for electric, hybrid, and plug-in hybrid electric vehicles," *IEEE Trans. Power Electron.*, vol. 27, no. 1, pp. 122–132, Jan. 2012.

[58] Y. Tang, P. C. Loh, P. Wang, F. H. Choo, F. Gao, and F. Blaabjerg, "Generalized design of high performance shunt active power filter with output LCL filter," *IEEE Trans. Ind. Electron.*, vol. 59, no. 3, pp. 1443–1452, Mar. 2012.

[59] S. B. Karanki, N. Geddada, M. K. Mishra, and B. K. Kumar, "A DSTATCOM topology with reduced DC-link voltage rating for load compensation with nonstiff source," *IEEE Trans. Power Electron.*, vol. 27, no. 3, pp. 1201–1211, Mar. 2012.

[60] N. Flourentzou, V. G. Agelidis, and G. D. Demetriades, "VSC-based HVDC power transmission systems: An overview," *IEEE Trans. Power Electron.*, vol. 24, no. 3, pp. 592–602, Mar. 2009.

[61] J. G. Kassakian and T. M. Jahns, "Evolving and emerging applications of power electronics in systems," *IEEE J. Emerg. Sel. Topics Power Electron.*, vol. 1, no. 2, pp. 47–58, Jun. 2013.

[62] S. Yang, J. Fang, Y. Tang, and P. Wang, "Synthetic-inertia-based modular multilevel converter frequency control for improved microgrid frequency regulation," in *Proc. IEEE ECCE*, Portland, OR, USA, Sep. 2018, pp. 23–27.

[63] D. G. Holmes and T. A. Lipo, *Pulse Width Modulation for Power Converters: Principles and Practice*. Hoboken, NJ, USA: Wiley, 2003.

[64] J. Fang, X. Li, Y. Tang, and H. Li, "Design of virtual synchronous generators with enhanced frequency regulation and reduced voltage distortions," in *Proc. IEEE APEC*, San Antonio, TX, USA, Mar. 2018, pp. 1–8.

[65] J. Fang, Y. Tang, H. Li, and X. Li, "A battery/ultracapacitor hybrid energy storage system for implementing the power management of virtual synchronous generators," *IEEE Trans. Power Electron.*, vol. 33, no. 4, pp. 2820–2824, Apr. 2018.

[66] R. W. Erickson and D. Maksimovic, *Fundamentals of Power Electronics*. New York, NY, USA: Springer, 2001.

[67] *Enhanced Frequency Response*, Nat. Grid, London, U.K., 2017. [Online]. Available: http://www2.nationalgrid.com

[68] *Providing Flexibility With a Virtual Power Plant—Final Demo Report*, DONG Energy, Fredericia, Denmark, 2013. [Online]. Available: https://www.slideshare.net

[69] L. A. Roberto, "2013 JRC wind status repot—Technology, market and economic aspects of wind energy in Europe," EU Science Hub, Petten, The Netherlands, Tech. Rep., 2013. [Online]. Available: http://iet.jrc.ec.europa.eu, doi: 10.2790/97044.

[70] Z. Xin, P. Loh, X. Wang, F. Blaabjerg, and Y. Tang, "Highly accurate derivatives for LCL-filtered grid converter with capacitor voltage active damping," *IEEE Trans. Power Electron.*, vol. 31, no. 5, pp. 3612–3625, May 2016.

[71] Z. Xin, X. Wang, P. C. Loh, and F. Blaabjerg, "Realization of digital differentiator using generalized integrator for power converters," *IEEE Trans. Power Electron.*, vol. 30, no. 12, pp. 6520–6523, Dec. 2015.

[72] P. Rodriguez, A. Luna, M. Ciobotaru, R. Teodorescu, and F. Blaabjerg, "Advanced grid synchronization system for power converters under unbalanced and distorted operating conditions," in *Proc. 32nd Annu. Conf. IEEE Ind. Electron. (IECON)*, Nov. 2006, pp. 5173–5178.

[73] P. Rodríguez, A. Luna, R. S. Muñoz-Aguilar, I. Etxeberria-Otadui, R. Teodorescu, and F. Blaabjerg, "A stationary reference frame grid synchronization system for three-phase grid-connected power converters under adverse grid conditions," *IEEE Trans. Power Electron.*, vol. 27, no. 1, pp. 99–112, Jan. 2012.

[74] J. Fang, R. Zhang, H. Li, and Y. Tang, "Frequency derivative-based inertia enhancement by grid-connected power converters with a frequency-locked-loop," *IEEE Trans. Smart Grid*, to be published.

[75] D. Duckwitz and B. Fischer, "Modeling and design of df/dt-based inertia control for power converters," *IEEE J. Emerg. Sel. Topics Power Electron.*, vol. 5, no. 4, pp. 1553–1564, Dec. 2017.

[76] H.-P. Beck and R. Hesse, "Virtual synchronous machine," in *Proc. 9th Int. Conf. Elect. Power Quality Utilisation*, Barcelona, Spain, Oct. 2007, pp. 1–6.

[77] J. Driesen and K. Visscher, "Virtual synchronous generators," in *Proc. IEEE Convers. Del. Elect. Energy 21st Century Power Energy Soc. General Meeting*, Jul. 2008, pp. 1–3.

[78] Q.-C. Zhong and G. Weiss, "Synchronverters: Inverters that mimic synchronous generators," *IEEE Trans. Ind. Electron.*, vol. 58, no. 4, pp. 1259–1267, Apr. 2011.

[79] Y. Chen, R. Hesse, D. Turschner, and H.-P. Beck, "Improving the grid power quality using virtual synchronous machines," in *Proc. POWERENG*, Malaga, Spain, May 2011, pp. 1–6.

[80] Y. Chen, R. Hesse, D. Turschner, and H.-P. Beck, "Investigation of the Virtual Synchronous Machine in the island mode," in *Proc. ISGT Eur.*, Malaga, Spain, Oct. 2012, pp. 1–6.

[81] Q.-C. Zhong, P.-L. Nguyen, Z. Ma, and W. Sheng, "Self-synchronized synchronverters: Inverters without a dedicated synchronization unit," *IEEE Trans. Power Electron.*, vol. 29, no. 2, pp. 617–630, Feb. 2014.

[82] Q.-C. Zhong, "Power-electronics-enabled autonomous power systems: Architecture and technical routes," *IEEE Trans. Ind. Electron.*, vol. 64, no. 7, pp. 5907–5918, Jul. 2017.

[83] O. Mo, S. D'Arco, and J. A. Suul, "Evaluation of virtual synchronous machines with dynamic or quasi-stationary machine models," *IEEE Trans. Ind. Electron.*, vol. 64, no. 7, pp. 5952–5962, Jul. 2017.

[84] S. D'Arco and J. A. Suul, "Equivalence of virtual synchronous machines and frequency-droops for converter-based microgrids," *IEEE Trans. Smart Grid*, vol. 5, no. 1, pp. 394–395, Jan. 2014.

[85] S. D'Arco and J. A. Suul, "Virtual synchronous machines—Classification of implementations and analysis of equivalence to droop controllers for microgrids," in *Proc. IEEE Grenoble Conf.*, Grenoble, France, Jun. 2013, pp. 1–7.

[86] J. Liu, Y. Miura, and T. Ise, "Comparison of dynamic characteristics between virtual synchronous generator and droop control in inverter-based distributed generators," *IEEE Trans. Power Electron.*, vol. 31, no. 5, pp. 3600–3611, May 2016.

[87] J. A. Suul, S. D'Arco, and G. Guidi, "Virtual synchronous machine-based control of a single-phase bi-directional battery charger for providing vehicle-to-grid services," *IEEE Trans. Ind. Appl.*, vol. 52, no. 4, pp. 3234–3244, Jul./Aug. 2016.

[88] H. Wu *et al.*, "Small-signal modeling and parameters design for virtual synchronous generators," *IEEE Trans. Ind. Electron.*, vol. 63, no. 7, pp. 4292–4303, Jul. 2016.

[89] J. Liu, Y. Miura, H. Bevrani, and T. Ise, "Enhanced virtual synchronous generator control for parallel inverters in microgrids," *IEEE Trans. Smart Grid*, vol. 8, no. 5, pp. 2268–2277, Sep. 2017.

[90] Y. Hirase, K. Sugimoto, K. Sakimoto, and T. Ise, "Analysis of resonance in microgrids and effects of system frequency stabilization using a virtual synchronous generator," *IEEE J. Emerg. Sel. Topics Power Electron.*, vol. 4, no. 4, pp. 1287–1298, Dec. 2016.

[91] P. F. Frack, P. E. Mercado, M. G. Molina, E. H. Watanabe, R. W. De Doncker, and H. Stagge, "Control strategy for frequency control in autonomous microgrids," *IEEE J. Emerg. Sel. Topics Power Electron.*, vol. 3, no. 4, pp. 1046–1055, Dec. 2015.

[92] M. Ashabani and Y. A.-R. I. Mohamed, "Integrating VSCs to weak grids by nonlinear power damping controller with self-synchronization capability," *IEEE Trans. Power Syst.*, vol. 29, no. 2, pp. 805–814, Mar. 2014.

[93] H. A. Alsiraji and R. El-Shatshat, "Comprehensive assessment of virtual synchronous machine based voltage source converter controllers," *IET Gener., Transmiss. Distrib.*, vol. 11, no. 7, pp. 1762–1769, May 2017.

[94] M. Guan, W. Pan, J. Zhang, Q. Hao, J. Cheng, and X. Zheng, "Synchronous generator emulation control strategy for voltage source converter (VSC) stations," *IEEE Trans. Power Syst.*, vol. 30, no. 6, pp. 3093–3101, Nov. 2015.

[95] W. Wu *et al.*, "A virtual inertia control strategy for DC microgrids analogized with virtual synchronous machines," *IEEE Trans. Ind. Electron.*, vol. 64, no. 7, pp. 6005–6016, Jul. 2017.

[96] L. Xiong *et al.*, "Static synchronous generator model: A new perspective to investigate dynamic characteristics and stability issues of grid-tied PWM inverter," *IEEE Trans. Power Electron.*, vol. 31, no. 9, pp. 6264–6280, Sep. 2016.
[97] M. Ashabani and Y. A.-R. I. Mohamed, "Novel comprehensive control framework for incorporating VSCs to smart power grids using bidirectional synchronous-VSC," *IEEE Trans. Power Syst.*, vol. 29, no. 2, pp. 943–957, Mar. 2014.
[98] L. Huang *et al.*, "A virtual synchronous control for voltage-source converters utilizing dynamics of DC-link capacitor to realize self-synchronization," *IEEE J. Emerg. Sel. Topics Power Electron.*, vol. 5, no. 4, pp. 1565–1577, Dec. 2017.
[99] A. F. Hoke, M. Shirazi, S. Chakraborty, E. Muljadi, and D. Maksimovic, "Rapid active power control of photovoltaic systems for grid frequency support," *IEEE J. Emerg. Sel. Topics Power Electron.*, vol. 5, no. 3, pp. 1154–1163, Sep. 2017.
[100] J. Fang, X. Li, Y. Tang, and L. Hongchang, "Improvement of frequency stability in power electronics-based power systems," in *Proc. ACEPT*, Singapore, Oct. 2017, pp. 1–6.
[101] J. M. Guerrero, M. Chandorkar, T.-L. Lee, and P. C. Loh, "Advanced control architectures for intelligent microgrids—Part I: Decentralized and hierarchical control," *IEEE Trans. Ind. Electron.*, vol. 60, no. 4, pp. 1254–1262, Apr. 2013.
[102] A. Sangwongwanich, Y. Yang, and F. Blaabjerg, "High-performance constant power generation in grid-connected PV systems," *IEEE Trans. Power Electron.*, vol. 31, no. 3, pp. 1822–1825, Mar. 2016.
[103] A. Sangwongwanich, Y. Yang, F. Blaabjerg, and H. Wang, "Benchmarking of constant power generation strategies for single-phase grid-connected Photovoltaic systems," *IEEE Ind. Appl. Mag.*, vol. 54, no. 1, pp. 447–457, Jan./Feb. 2018.
[104] J. Alipoor, Y. Miura, and T. Ise, "Power system stabilization using virtual synchronous generator with alternating moment of inertia," *IEEE J. Emerg. Sel. Topics Power Electron.*, vol. 3, no. 2, pp. 451–458, Jun. 2015.
[105] D. Li, Q. Zhu, S. Lin, and X. Y. Bian, "A self-adaptive inertia and damping combination control of VSG to support frequency stability," *IEEE Trans. Energy Convers.*, vol. 32, no. 1, pp. 397–398, Mar. 2017.
[106] M. A. Torres L., L. A. C. Lopes, L. A. Morán T., and J. R. Espinoza C., "Self-tuning virtual synchronous machine: A control strategy for energy storage systems to support dynamic frequency control," *IEEE Trans. Energy Convers.*, vol. 29, no. 4, pp. 833–840, Dec. 2014.
[107] T. S. Borsche, T. Liu, and D. J. Hill, "Effects of rotational Inertia on power system damping and frequency transients," in *Proc. 54th IEEE Conf. Decis. Control*, Dec. 2015, pp. 5940–5946.
[108] B. K. Poolla, S. Bolognani, and F. Dörfler, "Optimal placement of virtual inertia in power grids," *IEEE Trans. Autom. Control*, vol. 62, no. 12, pp. 6209–6220, Dec. 2017.
[109] E. Ela, V. Gevorgian, A. Tuohy, B. Kirby, M. Milligan, and M. O'Malley, "Market designs for the primary frequency response ancillary service—Part I: Motivation and design," *IEEE Trans. Power Sys.*, vol. 29, no. 1, pp. 421–431, Jan. 2014.
[110] E. Ela, V. Gevorgian, A. Tuohy, B. Kirby, M. Milligan, and M. O'Malley, "Market designs for the primary frequency response ancillary service—Part II: Case studies," *IEEE Trans. Power Syst.*, vol. 29, no. 1, pp. 432–440, Jan. 2014.
[111] Y. Liu, S. You, and Y. Liu, "Study of wind and PV frequency control in U.S. power grids—EI and TI case studies," *IEEE Power Energy Technol. Syst. J.*, vol. 4, no. 3, pp. 65–73, Sep. 2017.
[112] J. Rocabert, A. Luna, F. Blaabjerg, and P. Rodriguez, "Control of power converters in AC microgrids," *IEEE Trans. Power Electron.*, vol. 27, no. 11, pp. 4734–4749, Nov. 2012.
[113] J. M. Guerrero, J. C. Vasquez, J. Matas, L. G. de Vicuna, and M. Castilla, "Hierarchical control of droop-controlled AC and DC microgrids—A general approach toward standardization," *IEEE Trans. Ind. Electron.*, vol. 58, no. 1, pp. 158–172, Jan. 2011.
[114] P. C. Loh, D. Li, Y. K. Chai, and F. Blaabjerg, "Autonomous operation of hybrid microgrid with ac and dc subgrids," *IEEE Trans. Power Electron.*, vol. 28, no. 5, pp. 2214–2223, May 2013.
[115] F. Blaabjerg, Y. Yang, D. Yang, and X. Wang, "Distributed power-generation systems and protection," *IEEE Proc.*, vol. 105, no. 7, pp. 1311–1331, Jul. 2017.
[116] J. Fang, H. Li, Y. Tang, and F. Blaabjerg, "The role of power electronics in future low inertia power systems," in *Proc. IEEE PEAC*, Shenzhen, China, Nov. 2018, pp. 4–7.

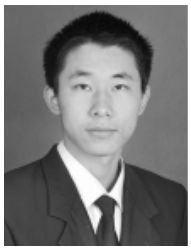

Jingyang Fang (S'15) received the B.Sc. and M.Sc. degrees in electrical engineering from Xi'an Jiaotong University, Xi'an, China, in 2013 and 2015, respectively. He is currently pursuing the Ph.D. degree at Nanyang Technological University, Singapore.

In 2018, he joined the Institute of Energy Technology, Aalborg University, Aalborg, Denmark, as a Visiting Scholar. He has authored and co-authored over 40 papers in the fields of power electronics and its applications, including 15 top-tier journal papers. His current research interests include power quality control, stability analysis and improvement, renewable energy integration, and digital control in more-electronics power systems.

Mr. Fang was a recipient of the Best Paper Award of Asia Conference on Energy, Power, and Transportation Electrification in 2017.

Hongchang Li (S'12−M'16) received the B.Eng. and D.Eng. degrees in electrical engineering from Xi'an Jiaotong University, Xi'an, China, in 2011 and 2016, respectively.

From 2014 to 2015, he was a Visiting Scholar with the Molecular Foundry, Lawrence Berkeley National Laboratory, Berkeley, CA, USA. He is currently a Research Fellow with the Energy Research Institute, Nanyang Technological University, Singapore. His current research interests include wireless power transfer, electron tomography, and distributed energy storage systems.

Yi Tang (S'10−M'14−SM'18) received the B.Eng. degree in electrical engineering from Wuhan University, Wuhan, China, in 2007, and the M.Sc. and Ph.D. degrees from the School of Electrical and Electronic Engineering, Nanyang Technological University, Singapore, in 2008 and 2011, respectively.

From 2011 to 2013, he was a Senior Application Engineer with Infineon Technologies Asia Pacific, Singapore. From 2013 to 2015, he was a Post-Doctoral Research Fellow with Aalborg University, Aalborg, Denmark. Since 2015, he has been an Assistant Professor with Nanyang Technological University, Singapore, where he is currently the Cluster Director of the Advanced Power Electronics Research Program with the Energy Research Institute.

Dr. Tang was a recipient of the Infineon Top Inventor Award in 2012, the Early Career Teaching Excellence Award in 2017, and four IEEE prize paper awards. He serves as an Associate Editor for the IEEE TRANSACTIONS ON POWER ELECTRONICS and the IEEE JOURNAL OF EMERGING AND SELECTED TOPICS IN POWER ELECTRONICS.

Frede Blaabjerg (S'86–M'88–SM'97–F'03) received the Ph.D. degree from Aalborg University, Aalborg, Denmark, in 1992.

From 1987 to 1988, he was with ABB-Scandia, Randers, Denmark. He was with Aalborg University, as an Assistant Professor in 1992, an Associate Professor in 1996, and a Full Professor of power electronics and drives in 1998. Since 2017, he has been a Villum Investigator. He holds an Honoris Causa doctorate at University Politehnica Timisoara, Timisoara, Romania, and Tallinn Technical University, Tallinn, Estonia. He has authored or co-authored over 600 journal papers in the fields of power electronics and its applications. He has co-authored four monographs and edited 10 books in power electronics and its applications. His current research interests include power electronics and its applications, such as in wind turbines, photovoltaic systems, reliability, harmonics, and adjustable speed drives.

Dr. Blaabjerg was a recipient of 28 IEEE prize paper awards, the IEEE PELS Distinguished Service Award in 2009, the EPE-PEMC Council Award in 2010, the IEEE William E. Newell Power Electronics Award in 2014, and the Villum Kann Rasmussen Research Award in 2014. He was the Editor-in-Chief of the IEEE TRANSACTIONS ON POWER ELECTRONICS from 2006 to 2012. He has been the Distinguished Lecturer of the IEEE Power Electronics Society from 2005 to 2007 and the IEEE Industry Applications Society from 2010 to 2011 and 2017 to 2018. He is currently the President Elect of the IEEE Power Electronics Society. He serves as the Vice President of the Danish Academy of Technical Sciences. He was nominated in 2014, 2015, 2016, and 2017 by Thomson Reuters to be among the 250 most cited researchers in engineering in the world.